Calculation of (K^-,π) hypernuclear yields for stopped kaons in ^{12}C

A. Gal*

TRIUMF, Vancouver, British Columbia, Canada V6T 2A3

L. Klieb

The Hebrew University, Jerusalem 91904, Israel
and Fundamenteel Onderzoek der Materie-Institute for Plasma Physics, Nieuwegein, The Netherlands
(Received 27 March 1986)

Yields of the ^{12}C(K$^-$, π^-)$^{12}_\Lambda$C and ^{12}C(K$^-$,π^+)$^{12}_\Sigma$Be stopped-kaon reactions to $1s$ and $1p$ hypernuclear states are studied in detail within the distorted wave impulse approximation, employing realistic K$^-$ atomic wave functions and pion distorted waves. The calculated Λ-hypernuclear yields are weaker than the Σ-hypernuclear yields by more than an order of magnitude, particularly because the outgoing pion wave is strongly damped in the Λ production region due to the proximity to the 3,3 resonance, and are sensitive to within factors of 1.5–3 to the choice of pion optical potential. The largest uncertainty, by as much as a factor of 3.5, is that for the ratio of 2^+ to 0^+ excitations. The calculated Σ-hypernuclear yields, on the other hand, are generally stable, to within 20%, to variations in the input parameters. The results of the calculation are compared with old and new data of stopped-kaon reactions on ^{12}C, and with previous theoretical reports. Yields are also calculated for production of $1p_\Lambda$ states in $^{16}_\Lambda$O which decay only by proton emission.

I. INTRODUCTION

The recent observation[1] of Σ-hypernuclear peaks in the reaction

$$^{12}\text{C}(\text{K}^-,\pi^+)^{12}_\Sigma\text{Be} \tag{1}$$

with stopped kaons has stimulated a renewed interest[2] in the seemingly outdated technique of capture from rest. The formation rates for these peaks total about 1% per stopped kaon, substantially higher—by more than an order of magnitude—than the rates previously measured[3] for peaks in the
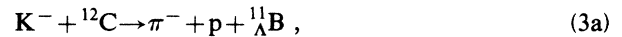
$$^{12}\text{C}(\text{K}^-,\pi^-)^{12}_\Lambda\text{C} \tag{2}$$

reaction. The prospects of establishing Λ- and Σ-hypernuclear spectroscopy in K$^-$ capture from rest have been pointed out by Yamazaki *et al.*[4] and by Tamura *et al.*,[5] and the corresponding issues for $^{12}_\Sigma$Be, the extraction of the Σ-nuclear spin-orbit coupling in particular, have been discussed in detail by Zofka[6] and by Dover *et al.*[7] The last comprehensive summary[8] of the experimental situation in this field has just appeared, during writing this work.

Hüfner *et al.*[9] formulated the distorted wave impulse approximation (DWIA) for (K^-,π) reactions both for stopped kaons and kaons in flight, and applied it to the formation of $^{12}_\Lambda$C. The present formulation of stopped-kaon reactions in Sec. II, although following the physics principles inherent in these original papers,[9] parallels closely in technique and appearance the spectroscopic study by Auerbach *et al.*[10] of (K^-,π^-) in flight to the Λ-hypernuclear region and that of the forthcoming spectroscopic analysis of Dover, Gal, and Millener[11] of (K^-,π) to the Σ-hypernuclear region. It is therefore quite

natural to inject the hypernuclear yields calculated here to these spectroscopic studies, as was recently done in Ref. 7. Furthermore, since the formalism presented in this work offers a correct treatment of charge degrees of freedom in the (K^-,π^-) reaction to the Σ-hypernuclear region, via a consistent usage of the isospin basis in both structure and reaction parts of the analysis, we are able to comment on some subtle issues arising in the interpretation of the $^{12}_\Sigma$C spectrum.[8]

In Secs. III, IV, and V we report an updated calculation and detailed study of hypernuclear formation rates in ^{12}C, reactions (1) and (2), and record some results for $^{16}_\Lambda$O. The calculation employs realistic K$^-$ atomic wave functions and pion distorted waves, thereby allowing a study of several sensitivities that have gone unnoticed, particularly for Λ hypernuclei, where the distortion of the outgoing pion [with momentum $q(\pi^-)\sim260$ MeV/c, close to the 3,3 resonance] is substantial. Such a study becomes particularly important when evaluating the very recent reappraisal[12] of older emulsion data[13] for the exclusive stopped-kaon reactions

$$\text{K}^- + {}^{12}\text{C} \rightarrow \pi^- + \text{p} + {}^{11}_\Lambda\text{B} , \tag{3a}$$

$$\text{K}^- + {}^{16}\text{O} \rightarrow \pi^- + \text{p} + {}^{15}_\Lambda\text{N} . \tag{3b}$$

Due to the fine resolution, as small as 50 keV for reaction (3a), the reconstructed π^- spectrum of these reactions shows evidence for several well resolved $^{12}_\Lambda$C* levels and possible $^{16}_\Lambda$O* levels, respectively. A reliable calculation of these hypernuclear yields, clearly, is a prerequisite for deriving spectroscopic information from these interesting spectra. Our calculated rates for $^{12}_\Lambda$C are smaller by about a factor of 2 from those reported in Refs. 9 and 14; we comment on these discrepancies.

Our calculations for $^{12}_\Sigma$Be extend those reported in Refs.

4 and 14 by considering p→Σ⁻ transitions from the proton $1p$ shell to the Σ^- $1d_j$ subshells. This may become relevant in seeking an explanation for the appearance of a relatively narrow peak about 11 MeV in the Σ^- continuum for stopped kaons[2,8] and, perhaps, also in flight.[15] Where comparison is possible, our calculated yields agree with the data[1,8] but disagree by factors of 2−3 with those reported in the calculation by Matsuyama and Yazaki.[14] We comment on these discrepancies. Preliminary, partial results of the present calculation were reported in Ref. 16.

II. FORMALISM

The capture rate for the reaction

$$K^- + A\,(i) \to \pi^{-\tau-1/2} + H\,(f) \tag{4}$$

at rest, where $-\tau-\frac{1}{2}$ is the pion charge, A is the target nucleus in initial state i, and H is the (Λ or Σ) hypernucleus in the final state f, is given by (in units $\hbar=c=1$)

$$\Gamma_{if} = 2\pi \int \delta(E_\pi + E_H - E_{K^-} - E_A) \langle \,|\,T_{if}(\mathbf{q})\,|^2 \rangle \frac{d^3q}{(2\pi)^3}$$

$$= (2\pi)^{-2} q_f \omega_f \int \langle \,|\,T_{if}(\mathbf{q}_f)\,|^2 \rangle d\Omega_{q_f} \,. \tag{5}$$

$$\rho_{if}(\mathbf{r}) = \left\langle \alpha_f J_f M_f; T_f t_f \left| \sum_{\alpha,\beta} \psi_\beta^{Y*}(\mathbf{r}) \psi_\alpha^N(\mathbf{r}) a_Y^\dagger(\beta) a_N(\alpha) \right| \alpha_i J_i M_i; T_i t_i \right\rangle \tag{8}$$

over the kaon initial wave function and the pion distorted wave:

$$\tilde{\rho}_{if}^{DW}(\mathbf{q}_f) = \int \chi_{q_f}^{(-)*}(\mathbf{r}) \rho_{if}(\mathbf{r}) \Psi_{nLM}(\mathbf{r}) d^3r \,. \tag{9}$$

The subscripts α and β in the nucleon wave function ψ^N and the hyperon wave function ψ^Y, respectively, run over complete sets of single-particle states, and $a_Y^\dagger(\beta), a_N(\alpha)$ are creation and annihilation operators, respectively, for these states. The K^- atomic wave function Ψ_{nLM} is obtained by solving the Klein-Gordon equation for the negatively charged kaon in the Coulomb orbit (n,L) due to the nuclear charge distribution with a full consideration of the K^--nuclear strong-interaction optical potential; the latter is assumed to be proportional to the nuclear density with a (complex) depth required to fit the measured energy shifts and widths of the K^- atomic levels. The pion distorted wave $\chi_q^{(-)}$ in the final state is given in terms of the partial-wave expansion

$$\chi_q^{(-)*}(\mathbf{r}) = \chi_{-q}^{(+)}(\mathbf{r}) = \sum_l i^{-l}(2l+1)\tilde{j}_l(r) P_l(\hat{\mathbf{q}}\cdot\hat{\mathbf{r}}) \,. \tag{10}$$

The radial wave function $\tilde{j}_l$, reducing to the spherical Bessel function $j_l(qr)$ for a free pion, solves the Klein-Gordon equation with the pion-nuclear strong-interaction optical potential plus the appropriate Coulomb field of the nucleus.

Using the relationship between t and the in-medium two-body scattering amplitude f,

$$(\bar{\omega}_i \bar{\omega}_f)^{1/2} t(\bar{q}_f) = -2\pi \bar{f} \,, \tag{11}$$

Here the $\langle \ \rangle$ mean that the square of the T matrix for this process is averaged on the initial M states and summed over the final ones. The momentum q_f of the outgoing pion is determined by the energy-conserving δ function, and ω_f is the reduced energy in the final state,

$$\omega_f^{-1} = E_\pi^{-1}(q_f) + E_H^{-1}(q_f); \quad \omega_f \to E_\pi(q_f) \quad \text{for } A \to \infty \,.$$

A. Formulation of the DWIA

In the DWIA, the (K^-,π) reaction (4) is driven by the one-baryon reaction

$$K^- + N \to \pi^{-\tau-1/2} + Y \quad (Y=\Lambda,\Sigma) \tag{6}$$

on nucleon N, with the in-medium T matrix denoted by t, assumed here to be of the s-wave type:

$$T_{if}(\mathbf{q}_f) = \sum_{j=1}^N \langle f\,|\,t_j(\mathbf{q}_f)\,|\,i \rangle_{DW} = t(q_f)\tilde{\rho}_{if}^{DW}(\mathbf{q}_f) \,. \tag{7}$$

The charge indices were omitted in (7) for simplicity (the appropriate generalization is deferred to subsection C below). The superscript DW stands for integrating the transition density

and singling out the combination appropriate to the in-medium two-body capture rate,

$$\bar{\gamma} \equiv \bar{v}_i \bar{\sigma} = 4\pi(\bar{q}_f/\bar{\omega}_i)\,|\,\bar{f}\,|^2 \,, \tag{12}$$

where $v_i = q_i/\omega_i$, σ is the cross section for reaction (6), and $\bar{\omega}_i, \bar{\omega}_f, \bar{q}_f$ are appropriately averaged in-medium quantities, we finally reach the DWIA expression for the capture rate (5):

$$\Gamma_{if} = (q_f \omega_f / \bar{q}_f \bar{\omega}_f) \bar{\gamma} \int \langle \,|\,\tilde{\rho}_{if}^{DW}(\mathbf{q}_f)\,|^2 \rangle d\Omega_{q_f}/4\pi \,. \tag{13}$$

A sensible choice of $\bar{q}_f$ would be the pion momentum at the peak of the quasifree spectrum; the kinematical factor $(q_f \omega_f / \bar{q}_f \bar{\omega}_f)$ can then be approximated by unity when summing over all final states.

B. Sum rule and rate per stopped K^-

Neglecting the q_f dependence of the pion distorted wave, replacing it by $\bar{q}_f$, and recalling Eq. (9) for $\tilde{\rho}_{if}^{DW}(\mathbf{q}_f)$, the summation over all final hypernuclear states in (13) is accomplished by applying closure:

$$\frac{1}{2J_i+1} \sum_{M_i} \sum_f \rho_{fi}^*(\mathbf{r}')\rho_{fi}(\mathbf{r}) = \rho_N(r)\delta(\mathbf{r}-\mathbf{r}') \,, \tag{14}$$

where $\rho_N(r)$ is the nuclear density of nucleon type N,

$$\int \rho_N(r) d^3r = N \,.$$

We thus obtain

$$\sum' \Gamma_{if} = \bar{\gamma} \int \rho_N(r)\rho_{K^-}(r)|X_{\bar{q}_f}(r)|^2 d^3r \ , \qquad (15)$$

where

$$\rho_{K^-}(r) = \frac{1}{2L+1}\sum_M |\Psi_{nLM}(\mathbf{r})|^2 = |R_{nL}(r)|^2/4\pi \ , \qquad (16)$$

$$\int \rho_{K^-}(r)d^3r = 1 \ ,$$

$$|X_q(r)|^2 = \int |X_q^{(-)}(\mathbf{r})|^2 d\Omega_q/4\pi$$

$$= \sum_l (2l+1)|\tilde{j}_l(r)|^2 \ , \qquad (17)$$

and the prime on the summation symbol denotes a restriction to the pion elastic scattering mode. To obtain an overall capture rate, regardless of the history of the final pion, whether it was elastically or inelastically scattered (with or without charge exchange), or genuinely absorbed, we relax this restriction rooted in the very formulation of the DWIA, replacing the distorted wave $X_q^{(-)^*}(\mathbf{r})$ by the free wave $\exp(-i\mathbf{q}\cdot\mathbf{r})$. Therefore,

$$\Gamma = \sum_f \Gamma_{if} = \bar{\gamma}\int \rho_N(r)\rho_{K^-}(r)d^3r \ , \qquad (18)$$

in agreement with the semiclassical expression

$$\Gamma = \bar{v}_i\bar{\sigma}(K^-N\rightarrow\pi Y)\bar{\rho}_N \ ,$$

provided definition (11) is recalled and $\bar{\rho}_N$—the effective nuclear density available to the capture process—is defined as

$$\bar{\rho}_N = \int \rho_N(r)\rho_{K^-}(r)d^3r \ . \qquad (19)$$

Expression (18) is readily generalized to account for K^- capture on both protons and neutrons. The nuclear capture rate through the mode (6) *per stopped K^-*, R/K^-, is then given by

$$R_{if}/K^- = \frac{\Gamma_{if}}{\Gamma} = (q_f\omega_f/\bar{q}_f\bar{\omega}_f)R\,(\pi^{-\tau-1/2}Y)$$

$$\times \frac{\int \langle |\bar{\rho}_{if}^{DW}(\mathbf{q}_f)|^2\rangle d\Omega_{q_f}/4\pi}{\bar{\rho}_N} \ , \qquad (20)$$

where the fractions

$$R\,(\pi^{-\tau-1/2}Y) = \frac{\bar{\gamma}(K^-N\rightarrow\pi^{-\tau-1/2}Y)\bar{\rho}_N}{\bar{\gamma}(K^-p\rightarrow\text{all})\bar{\rho}_p + \bar{\gamma}(K^-n\rightarrow\text{all})\bar{\rho}_n} \qquad (21)$$

are the primary branching ratios for mononucleonic K^- absorptions at rest in the nucleus considered. These fractions were determined in carbon nuclei of a heavy-liquid bubble chamber by Vander Velde-Wilquet et al.,[17] and tabulated in Table II there. We reproduce these values for charged pions in Table I, after adjusting them to account also for the 19% multinucleonic captures at rest. Values appropriate to heavy freon are included in the table in order to indicate the trend in going from light nuclei to heavy nuclei. One observes that (i) Σ^- production in (K^-,π^+) is rather stable, (ii) Σ^0 production in (K^-,π^-) remains suppressed throughout the Periodic Table, and (iii) Σ^+ and *direct* Λ production roughly trade off intensities. The values in Table I are quite different from those measured in hydrogen and extended via charge independence to give the branching rates for reactions (6) at rest on a free nucleon. This difference originates most likely from the increasing dominance of the $I=0$ $\Lambda(1405)$ resonance below threshold due to nuclear binding and, in heavy nuclei, perhaps also from the difference between proton and neutron densities in the tail region of the nucleus. We note that the primary branching ratios (21), to be used in the DWIA expression (20), correspond to the *production* stage, not to the *emission* stage in which many of the observed Λ hyperons are known to have resulted from Σ conversion. Indeed, the emission fraction of Λ following K^- absorptions in carbon nuclei was determined[18] in the same heavy-liquid bubble chamber to be as high as 0.68, with only 23% due to direct $\pi^-\Lambda$ production, as much as 64% due to conversion following $\pi^-\Sigma^+$ production, and 13% following $\pi^-\Sigma^0$ production.

The calculations reported in this paper were made for the last quantity on the right-hand side (rhs) of Eq. (20),

$$\frac{\int \langle |\bar{\rho}_{if}^{DW}(\mathbf{q}_f)|^2\rangle d\Omega_{q_f}/4\pi}{\bar{\rho}_N} = \frac{1}{(2L+1)(2J_i+1)}\sum_{MM_iM_f} \frac{\int d\Omega_{q_f}\left|\int X_{q_f}^{(-)^*}(\mathbf{r})\rho_{if}(\mathbf{r})\Psi_{nLM}(\mathbf{r})d^3r\right|^2}{4\pi\int \rho_N(r)\rho_{K^-}(r)d^3r} \ , \qquad (22)$$

TABLE I. K^- absorption fractions $R\,(\pi^{\pm}Y)$ for charged pions, Eq. (21), in carbon and freon (Ref. 17). These fractions were adjusted to account for multinucleonic captures as well.

Nuclear medium	$R\,(\pi^{\pm}Y)$			
	$K^-n\rightarrow\pi^-\Lambda$	$K^-p\rightarrow\pi^+\Sigma^-$	$K^-p\rightarrow\pi^-\Sigma^+$	$K^-n\rightarrow\pi^-\Sigma^0$
C	0.070	0.136	0.305	0.027
CF$_3$Br	0.237	0.111	0.113	0.032

TABLE II. $K^-N \to \pi Y$ amplitudes, Eq. (25), appropriate to the nuclear $(K^-,\pi^\pm)$ reactions. The isospin of the hyperon (Y) is t_Y, and (t,τ) are the isospin transfer and its z projection, respectively.

Nuclear reaction	t_Y	Y	t	τ	$\bar{f}^{t_Y}_{(t,\tau)}$
(K^-,π^-)	0	Λ^0	$\frac{1}{2}$	$\frac{1}{2}$	$-\bar{f}_{K^-n \to \pi^-\Lambda}$
	1	Σ^0, Σ^+	$\frac{1}{2}$	$\frac{1}{2}$	$(\frac{1}{3})^{1/2}\bar{f}_{K^-n \to \pi^-\Sigma^0} + (\frac{2}{3})^{1/2}\bar{f}_{K^-p \to \pi^-\Sigma^+}$
	1	Σ^0, Σ^+	$\frac{3}{2}$	$\frac{1}{2}$	$-(\frac{2}{3})^{1/2}\bar{f}_{K^-n \to \pi^-\Sigma^0} + (\frac{1}{3})^{1/2}\bar{f}_{K^-p \to \pi^-\Sigma^+}$
(K^-,π^+)	1	Σ^-	$\frac{3}{2}$	$-\frac{3}{2}$	$\bar{f}_{K^-p \to \pi^+\Sigma^-}$

which we loosely call R_{if}/Y, the *rate per hyperon* Y (with charged pion $\pi^{-\tau-1/2}$), because its derivation assumed that this capture mode (6) was the only available one. As noticed by previous authors,[9,14] the rhs of Eq. (22) is not very sensitive to the nuclear density and to the kaon orbit considered since these appear to the same power in both numerator and denominator. We find exceptions to this rule when the pion distortion, in the numerator, becomes substantial (Sec. III D below).

C. Extension to charge degrees of freedom

Equations (13) and (20) are sufficient for the evaluation of (K^-,π^+) yields, where—under the DWIA—capture occurs only on protons, and of (K^-,π^-) yields in the Λ-hypernuclear region where only neutrons are involved. However, an extension is required in the case of (K^-,π^-) reactions to the Σ-hypernuclear region, where the two elementary *primary* processes

$$K^-p \to \pi^-\Sigma^+, \quad K^-n \to \pi^-\Sigma^0$$

generally compete with each other. To this end we replace the factor $\bar{f}_N a^\dagger_Y a_N$ that, due to Eqs. (8), (9), (11), and (12), determines the charge dependence of the amplitude (7) by

$$\bar{f}_N a^\dagger_Y a_N \to \bar{f}_p a^\dagger_{t_Y,\tau+1/2} a_{1/2,1/2}$$

$$+ \bar{f}_n a^\dagger_{t_Y,\tau-1/2} a_{1/2,-1/2} , \tag{23}$$

where $\bar{f}_p$ and $\bar{f}_n$ are the in-medium two-body amplitudes for process (6) occurring on protons or neutrons, respectively. t_Y is the hyperon isospin, $t_\Lambda = 0$ and $t_\Sigma = 1$, and τ is the z component of isospin transfer from the nucleon to the hyperon; by charge conservation, $\tau = \frac{1}{2}$ for (K^-,π^-) and $-\frac{3}{2}$ for (K^-,π^+) reactions. Using a time-reversed construct

$$\tilde{a}_{1/2,1/2} = -a_{1/2,-1/2}, \quad \tilde{a}_{1/2,-1/2} = a_{1/2,1/2},$$

we rewrite Eq (23) as

$$\bar{f}_N a^\dagger_Y a_N \to \sum_{t=1/2,3/2} \bar{f}^{t_Y}_{(t,\tau)}(a^\dagger_{t_Y} \otimes \tilde{a}_{1/2})^t_\tau , \tag{24}$$

where t acquires the meaning of *isospin transfer*, with τ now becoming its z projection. The amplitudes $\bar{f}^{t_Y}_{(t,\tau)}$ constitute t-channel amplitudes

$$\bar{f}^{t_Y}_{(t,\tau)} = \sum_\lambda (\langle t_Y\lambda, \tfrac{1}{2} - \tfrac{1}{2} | t\tau\rangle \bar{f}_{p\to Y\lambda}$$

$$- \langle t_Y\lambda, \tfrac{1}{2}\tfrac{1}{2} | t\tau\rangle \bar{f}_{n\to Y\lambda}) \tag{25}$$

and are given in Table II in terms of the more familiar s-channel amplitudes. The DWIA expression (13) is now replaced by

$$\Gamma_{if} = (q_f\omega_f/\bar{\omega}_i\bar{\omega}_f)\tilde{\Gamma}_{if}$$

with

$$\tilde{\Gamma}_{if} = \int \left\langle \left| \sum_t \bar{f}^{t_Y}_{(t,\tau)}\tilde{\rho}^{(t,\tau)DW}_{t_Y,1/2}(q_f) \right|^2 \right\rangle d\Omega_{q_f} , \tag{26}$$

where

$$\tilde{\rho}^{(t,\tau)DW}_{t_Y,1/2}(q) = \int \chi^{(-)*}_q(r)\rho^{(t,\tau)}_{t_Y,1/2}(r)\Psi_{nLM}(r)d^3r , \tag{27}$$

$$\rho^{(t,\tau)}_{t_Y,1/2}(r) = \left\langle \alpha_f J_f M_f; T_f t_f \left| \sum_{\alpha,\beta} \psi^{Y*}_\beta(r)\psi^N_\alpha(r)[a^\dagger_{t_Y}(\beta) \otimes \tilde{a}_{1/2}(\alpha)]^t_\tau \right| \alpha_i J_i M_i; T_i t_i \right\rangle . \tag{28}$$

The generalization of the sum rule (14) is given by

$$\frac{1}{2J_i+1} \sum_{M_i} \sum_f \sum_{t,t'} \bar{f}^{t_Y*}_{(t',\tau)}\bar{f}^{t_Y}_{(t,\tau)}\rho^{(t',\tau)*}_{t_Y,1/2}(r')\rho^{(t,\tau)}_{t_Y,1/2}(r) = [|\bar{f}_{p\to Y^{\tau+1/2}}|^2\rho_p(r) + |\bar{f}_{n\to Y^{\tau-1/2}}|^2\rho_n(r)]\delta(r-r') , \tag{29}$$

justifying *a posteriori* the form of the denominator in Eq. (21) for $R(\pi^{-\tau-1/2}Y)$. Equation (20) for the rate per stopped K^-, for given τ and t_Y, now becomes

$$R_{if}/K^- = (q_f \omega_f / \bar{q}_f \bar{\omega}_f) \sum_\lambda R(\pi^{-\tau-1/2}Y^\lambda)$$

$$\times \frac{\int \left\langle \left| \sum_t \bar{f}^{t_Y}_{(t,\tau)} \tilde{\rho}^{(t,\tau)DW}_{t_Y,1/2}(q_f) \right|^2 \right\rangle d\Omega_{q_f}}{|\bar{f}_{p \to Y^{\tau+1/2}}|^2 \int \rho_p(r) |R_{nL}(r)|^2 d^3r + |\bar{f}_{n \to Y^{\tau-1/2}}|^2 \int \rho_n(r) |R_{nL}(r)|^2 d^3r} \ , \tag{30}$$

with

$$\sum_\lambda R(\pi^{-\tau-1/2}Y^\lambda) = \frac{\bar{\gamma}(K^-p \to \pi^{-\tau-1/2}Y^{\tau+1/2})\bar{\rho}_p + \bar{\gamma}(K^-n \to \pi^{-\tau-1/2}Y^{\tau-1/2})\bar{\rho}_n}{\bar{\gamma}(K^-p \to \text{all})\bar{\rho}_p + \bar{\gamma}(K^-n \to \text{all})\bar{\rho}_n} \ . \tag{31}$$

[The denominator in Eq. (31) is the same as in Eq. (21) and should also, in practice, include multinucleonic captures at rest as well.] Equations (30) and (31) provide the required extension for (K^-,π^-) reactions to the Σ-hypernuclear region $(t_Y = 1, \tau = \frac{1}{2})$.

D. Partial-wave analysis

The partial wave analysis of the partial rate $\tilde{\Gamma}_{if}$, Eq. (26), for use in Eq. (30), is accomplished along the same lines of the procedure adopted for (K^-,π) reactions in flight.[10,11] The single-particle wave functions ψ_α and ψ_β^* in the definition (28) of the isospin-labeled transition density $\rho^{(t,\tau)}_{t_Y,1/2}(r)$ are taken in the spherical basis,

$$\psi_{\gamma,m}(\mathbf{r}) = [u_{nlj}(r)/r][Y_l(\hat{r}) \otimes \chi_{1/2}]^j_m, \quad \gamma = \{nlj\}$$

and a time-reversed representation is adopted:

$$a_{jm} = (-1)^{j-m}\tilde{a}_{j,-m}, \quad \psi^*_{jm} = (-1)^{j+m}\bar{\psi}_{j,-m} \ . \tag{32}$$

The transition density becomes

$$\rho^{(t,\tau)}_{t_Y,1/2}(\mathbf{r}) = \sum_{\gamma_N,\gamma_Y} \sum_{k,m} (-1)^{k+m}[\psi_{\gamma_Y}(\mathbf{r}) \otimes \psi_{\gamma_N}(\mathbf{r})]^k_{-m}\rho^{(k,m)(t,\tau)}_{\gamma_Y t_Y, \gamma_N 1/2} \ , \tag{33}$$

$$\rho^{(k,m)(t,\tau)}_{\gamma_Y t_Y, \gamma_N 1/2} = (a^\dagger_{\gamma_Y t_Y} \otimes \tilde{a}_{\gamma_N 1/2})^{kt}_{m\tau} \ . \tag{34}$$

The summation over M_i and M_f, implicit in Eq. (26), can be carried out in closed form:

$$\tilde{\Gamma}_{if} = \frac{1}{(2L+1)(2J_i+1)} \sum_{k,m,M} \int d\Omega_{q_f} \left| \sum_{\gamma_N,\gamma_Y,t} \bar{f}^{t_Y}_{(t,\tau)}\beta^k_m(\gamma_Y,\gamma_N)\langle \alpha_f J_f; T_f t_f || \rho^{k(t,\tau)}_{\gamma_Y t_Y, \gamma_N 1/2} || \alpha_i J_i; T_i t_i \rangle \right|^2 \ , \tag{35}$$

where the matrix element is reduced[19] in J, but not in T, and the quantities $\beta^k_m(\gamma_Y,\gamma_N)$ are given by

$$\beta^k_m(\gamma_Y,\gamma_N) = (-1)^{k+m} \int \chi^{(-)*}_{q_f}(\mathbf{r})[\bar{\psi}_{\gamma_Y}(\mathbf{r}) \otimes \psi_{\gamma_N}(\mathbf{r})]^k_{-m}\Psi_{nLM}(\mathbf{r})d^3r \ , \tag{36}$$

in close similarity to the DW reduced amplitudes used by Auerbach et al.[10] The angular $\hat{q}_f$ integration is performed by utilizing the partial-wave expansion, Eq. (10), of the pion distorted wave and, subsequently, the angular $\hat{r}$ integration follows too. The net result is

$$\tilde{\Gamma}_{if} = \frac{1}{2J_i+1} \sum_{k,l} \langle L0,k0|l0 \rangle^2 \left| \sum_{\gamma_N,\gamma_Y,t} \bar{f}^{t_Y}_{(t,\tau)}I^{(l)}_{\gamma_Y,\gamma_N}(-1)^{1/2+j_N+l_Y} \right.$$

$$\times (2l_N+1)^{1/2}\langle l_N0,k0|l_Y0 \rangle[(2j_N+1)(2j_Y+1)]^{1/2} \begin{Bmatrix} j_Y & l_Y & 1/2 \\ l_N & j_N & k \end{Bmatrix}$$

$$\times \langle \alpha_f J_f; T_f t_f || \rho^{k(t,\tau)}_{\gamma_Y t_Y, \gamma_N 1/2} || \alpha_i J_i; T_i t_i \rangle \Bigg|^2 \ , \tag{37}$$

where the amplitudes

$$I^{(l)}_{\gamma_Y,\gamma_N} = \int_0^\infty \tilde{j}_l(r)u^*_{n_Y l_Y j_Y}(r)u_{n_N l_N j_N}(r)R_{nL}(r)dr \tag{38}$$

relate to the dynamics of the capture process. Expression (37) bears a striking similarity to Eq. (3.11) of Ref. 10 for (K^-,π) in flight, the only difference being the average taken here with squares of Clebsch-Gordan coefficients $\langle L0,k0|l0 \rangle^2$ over the l values permitted for given L and multipolarity k. When K^- capture from rest is considered

from a given $n_N l_N$ shell to a given $n_Y l_Y$ shell, the following simplifications occur.

(i) Sum over $\alpha_f J_f T_f$ of the hypernuclear $n_Y l_Y$ shell in order to find the overall strength of such a capture and to gauge the relative importance of the various operative multipolarities k. The result is

$$\tilde{\Gamma}_{n_N l_N \to n_Y l_Y} = \sum_{k, j_N, j_Y} (2l_N+1)\langle l_N 0, k 0 \mid l_Y 0 \rangle^2 (2j_Y+1)(2k+1) \begin{Bmatrix} l_Y & l_N & k \\ j_N & j_Y & 1/2 \end{Bmatrix}^2 N^{(k)}_{\gamma_Y, \gamma_N}$$

$$\times [Z(j_N) \mid \bar{f}_{p \to Y^{\tau+1/2}} \mid^2 + N(j_N) \mid \bar{f}_{n \to Y^{\tau-1/2}} \mid^2] , \qquad (39)$$

where

$$N^{(k)}_{\gamma_Y, \gamma_N} = \sum_l \langle L 0, k 0 \mid l 0 \rangle^2 \mid I^{(l)}_{\gamma_Y, \gamma_N} \mid^2 , \qquad (40)$$

and $Z(j_N)$ and $N(j_N)$ are the number of target protons and neutrons, respectively, in the j_N shell. The DWIA calculation modifies, thus, the capture rate for free nucleons (though with in-medium amplitudes $\bar{f}_N$) by multiplying it by

$$(2l_N+1)\langle l_N 0, k 0 \mid l_Y 0 \rangle^2 (2j_Y+1)$$

$$\times \sum_k (2k+1) \begin{Bmatrix} l_Y & l_N & k \\ j_N & j_Y & 1/2 \end{Bmatrix}^2 N^{(k)}_{\gamma_Y, \gamma_N} , \qquad (41)$$

for the $\gamma_N \to \gamma_Y$ transitions. This latter expression is tabulated in Table III for transitions of interest here. For capture at rest we find the integrals contributing to $N^{(k)}$ almost independent of the j quantum numbers (this depen-

dence enters through the difference in binding energies within a spin-orbit doublet for which the radial wave functions u_{nlj} are generated). Under these conditions, the total $\gamma_N \to \sum_{j_Y} \gamma_Y$ capture rate undergoes the nuclear modification

$$\sum_k (2k+1)\langle l_N 0, k 0 \mid l_Y 0 \rangle^2 N^{(k)}_{n_Y l_Y, n_N l_N} \qquad (42)$$

independent of j_N. Thus, the $1p_N \to 1p_Y$ rate is proportional to $N^{(0)}_{1p,1p} + 2N^{(2)}_{1p,1p}$; the $N^{(0)}_{1p,1p}$ term gives the strength of the summed 0^+ production and the $2N^{(2)}_{1p,1p}$ term gives the strength of the summed 2^+ production in ^{12}C.

(ii) If the amplitudes $I^{(l)}_{\gamma_Y, \gamma_N}$ are only weakly dependent on the j quantum numbers, one may reduce Eq. (37) further without summing over final states, by neglecting this dependence and working in the LS coupling basis:

$$\tilde{\Gamma}_{if} = \frac{2(2l_N+1)}{2J_i+1} \sum_k \langle l_N 0, k 0 \mid l_Y 0 \rangle^2 N^{(k)}_{n_Y l_Y, n_N l_N}$$

$$\times \left| \sum_t \bar{f}^{t_Y}_{(t,\tau)} \langle \alpha_f J_f; T_f t_f \mid\mid \rho^{(k_L=k, k_S=0)k,(t,\tau)}_{l_Y 1/2 t_Y, l_N 1/2 1/2} \mid\mid \alpha_i J_i; T_i t_i \rangle \right|^2 , \qquad (43)$$

where (suppressing the isospin labels) the LS density operator is defined as

$$\rho^{(k_L, k_S)k}_{l_Y 1/2, l_N 1/2} = [(a^\dagger_{n_Y l_Y} \otimes \tilde{a}_{n_N l_N})^{k_L} \otimes (a^\dagger_{1/2} \otimes \tilde{a}_{1/2})^{k_S}]^k .$$

E. Plane-wave results

In anticipation of the DWIA results (Sec. IV) for K^- capture from rest in ^{12}C, we offer some insight to the rates expected *per hyperon*, Eq. (22), by evaluating these in

the plane wave impulse approximation (PWIA) for pions of momentum q and assuming capture to occur from point Coulomb d ($L=2$) or p ($L=1$) orbits. The kaon wave functions are well approximated by r^L in the nucleus, and the baryons are assigned harmonic oscillator wave functions with a spring constant $\nu=0.37$ fm^{-2}. We evaluate the rates for transitions from the $1p$ protons *or* neutrons in ^{12}C to the summed $1s$ (1^- states) and the summed $1p$ (0^+ and 2^+ states) hyperon configurations, assuming one type of hyperon. The relevant expression is

TABLE III. The ratios given by Eq. (41) for K^--nuclear capture rates, transitions $\gamma_N \to \gamma_Y$, to capture rates on a free nucleon. The $N^{(k)}_{l_Y, l_N}$ are linear combinations of squares of DWIA integrals, as given in Eq. (40), which are assumed here to depend on l, not on j.

| Nuclear orbit | Y orbit | | | | |
	$1s_{1/2}$	$1p_{3/2}$	$1p_{1/2}$	$1d_{5/2}$	$1d_{3/2}$
$1s_{1/2}$	$N^{(0)}_{0,0}$				
$1p_{3/2}$	$N^{(1)}_{0,1}$	$N^{(0)}_{1,1} + N^{(2)}_{1,1}$	$N^{(2)}_{1,1}$	$\frac{9}{5}N^{(1)}_{2,1} + \frac{6}{5}N^{(3)}_{2,1}$	$\frac{1}{5}N^{(1)}_{2,1} + \frac{9}{5}N^{(3)}_{2,1}$
$1p_{1/2}$	$N^{(1)}_{0,1}$	$2N^{(2)}_{1,1}$	$N^{(0)}_{1,1}$	$3N^{(3)}_{2,1}$	$2N^{(1)}_{2,1}$

A. GAL AND L. KLIEB

TABLE IV. Summed $1s_Y(1^-)$ and $1p_Y(0^+,2^+)$ excitation rates per hyperon Y, Eq. (44), in K^- capture from atomic orbit (n,L) in ^{12}C calculated in the PWIA. The variable x is defined by $x = q^2/2\nu$.

| | | $(R/Y)_{PWIA}$ | |
L	1^-	0^+	2^+
1	$\frac{2}{39}(3-2x+x^2)e^{-x}$	$\frac{50}{117}x(1-\frac{1}{5}x)^2e^{-x}$	$\frac{4}{117}x(10-4x+x^2)e^{-x}$
2	$\frac{2}{255}x(10-4x+x^2)e^{-x}$	$\frac{98}{765}x^2(1-\frac{1}{7}x)^2e^{-x}$	$\frac{4}{765}(45-60x+40x^2-8x^3+x^4)e^{-x}$

$$R_{1p \to J^\pi}/Y = \frac{4(2J+1)\langle 10,J0 \mid l_Y 0 \rangle^2 N^{(J)}_{n_Y l_Y, 1p}}{\int \rho_N(r) \mid R_{nL}(r) \mid^2 d^3 r}, \tag{44}$$

in accordance with Eq. (42), with a nucleon density given by

$$\rho_N = (\nu/\pi)^{3/2}(2 + 4\frac{2}{3}\nu r^2)\exp(-\nu r^2). \tag{45}$$

The factor 4 in the numerator of (44) arises from the four $1p$ protons or neutrons.

Expression (44) is tabulated in Table IV and shown in Figs. 1 and 2 as a function of $x = q^2/2\nu$. The separate regions of q corresponding to Λ and Σ production are

denoted in the figures by arrows. As function of q, the dominant production for small values of q is to $J = L$ natural-parity hypernuclear states, but it is clear from the table that the depicted states are far from saturating the capture strength. The other transitions, vanishing in the limit $q \to 0$, reach a maximum rate for finite values of q, as shown by the figures, then follow the falloff expected of all transitions at large momentum transfer. In both Λ and Σ regions, the rate of the 1^- ground-state transition $1p_N \to 1s_Y$ is weaker than the combined $1p_N \to 1p_Y$ rate to the 0^+ and 2^+ excited configuration. The 2^+ summed rate is relatively strong in both regions, a feature in contrast with small angle (K^-,π) production in flight.

The departure from the PWIA calculation above is moderate for Σ production (less than 20% for $L = 2$ and less than a factor of 2 for $L = 1$), when the various approximations are removed, but substantial for Λ produc-
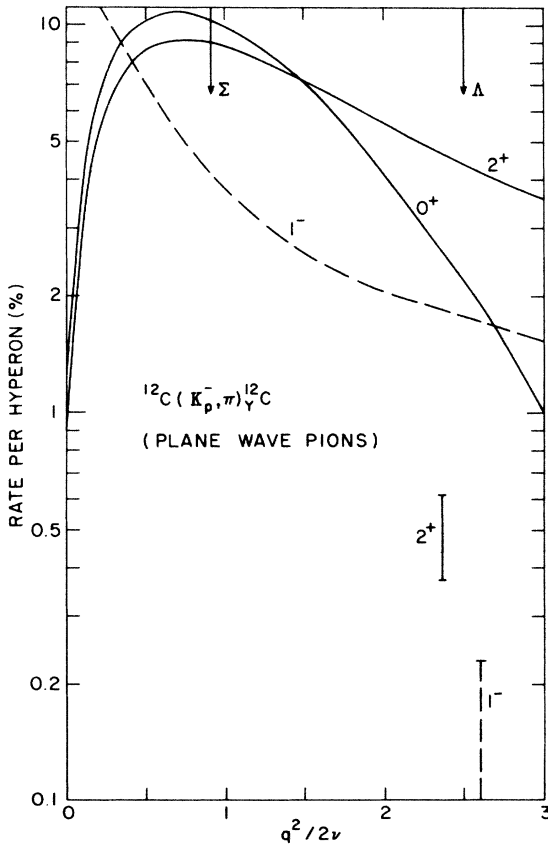

FIG. 1. Hypernuclear production rates calculated [Eq. (44) and Table IV] in the PWIA for the $1p(N) \to 1p(Y)$ 0^+ and 2^+, and for the $1p(N) \to 1s(Y)$ 1^- summed transitions in K^- capture from atomic p orbits in ^{12}C. The vertical bars show the marked effect of pion distortion for $^{12}_\Lambda C$ excitations in the DWIA.
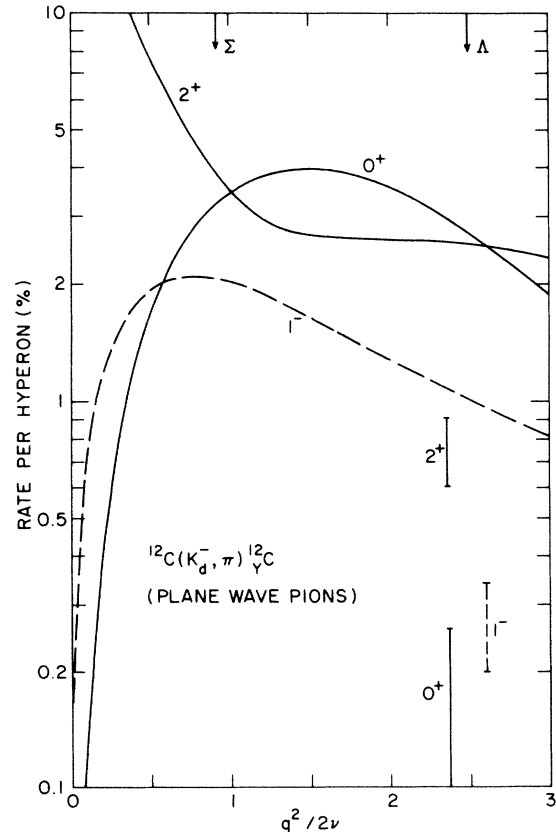

FIG. 2. Same as for Fig. 1, except that K^- capture occurs from atomic d orbits in ^{12}C.

tion. The DWIA results for Λ-hypernuclear production are marked in the figure by bars, the size of which is due to the sensitivity of the calculation to the pion optical potentials employed (as elaborated on in Sec. IV below). The main reason for the strong suppression in the DWIA is that pion-nuclear interactions in the Λ-production region are dominated by the 3,3 resonance. The strongest suppression occurs for the 0^+ rate which for $L=1$ (Fig. 1) does not even make it into the figure. Since K^- capture in ^{12}C occurs largely from d orbits, it is clear from Fig. 2, which shows almost equal rates for producing these Λ and Σ hypernuclear configurations in the PWIA, that pion absorption is the driving factor in weakening the Λ rates relative to the Σ rates by about an order of magnitude.

III. INPUT WAVE FUNCTIONS

This section provides a brief description of the input wave functions required for the DWIA calculation of K^- capture from rest in ^{12}C and ^{16}O to hypernuclear states. The DWIA amplitudes were defined in Sec. II by

$$I^{(l)}_{\gamma_Y,\gamma_N} = \int_0^\infty \tilde{j}_l(r) u^*_{n_Y l_Y j_Y}(r) u_{n_N l_N j_N}(r) R_{nL}(r) dr ,$$

(38)

where the $u_{nlj}(r)$ are the radial wave functions of the baryons generated here by Woods-Saxon real potentials to reproduce prescribed binding energies and/or rms radii, the $R_{nL}(r)$ are the radial wave functions of the K^- in atomic orbit (n,L), generated by a complex optical potential to reproduce given energy shifts and widths, and the $\tilde{j}_l(r)$ are the partial waves of the pion distorted waves constructed to fit measured elastic differential cross sections and total reaction cross sections. These DWIA amplitudes are then grouped together to form the quantities

$$N^{(k)}_{\gamma_Y,\gamma_N} = \sum_l \langle L\,0, k\,0 \mid l\,0 \rangle^2 \mid I^{(l)}_{\gamma_Y,\gamma_N} \mid^2$$

(40)

which appear in the numerator of expression (44) for the "rates per hyperon." The denominator of this expression [cf. Eqs. (16) and (19)],

$$4\pi\bar{\rho}_N = \int \rho_N(r) \mid R_{nL}(r) \mid^2 d^3r ,$$

(46)

can be constructed directly from the wave functions mentioned above by noting that

$$\rho_N(r) = \sum_{\gamma_N} N(j_N) u^2_{\gamma_N}(r) / 4\pi r^2 ,$$

$$\int \rho_N(r) d^3r = N ,$$

(47)

where the summation extends over all occupied orbits.

A. Kaon atomic wave functions and K^- capture

We follow the optical-model analysis of kaonic atoms reported by Batty.[20] The K^- optical potential is taken to be of the form

$$2\mu V^{K^-}_{opt}(r) = -4\pi(1+\mu/m)a\rho(r) ,$$

$$\int \rho(r) d^3r = A ,$$

(48)

where μ is the K^--nucleus reduced mass, m is the mass of the nucleon, $\rho(r)$ is the nucleon density (assuming equal proton and neutron distributions) identical in shape to the nuclear charge distribution,[21] and a is a complex effective scattering length. This optical potential is inserted into the Klein-Gordon equation together with the Coulomb potential due to the finite charge distribution of the nucleus and the first order $\alpha(Z\alpha)$ vacuum-polarization potential. The energy shift and width of the kaonic atom, and the corresponding complex wave function $R_{nL}(r)$, are then obtained by solving the radial equation to yield the complex eigenvalue energy of the bound kaon-nucleus system.[22] The real and imaginary parts of a are adjusted to fit the measured shifts and widths over some region of the Periodic Table. If shapes other than those for the nuclear charge distribution are assumed for $\rho(r)$, the emergent a's are different. We chose in our study two of the fitted scattering lengths,[20] as given in Table V. Choice (i) is natural to employ in the ^{12}C region, which we explore here, because it was obtained[20] by fitting to the measured $3\rightarrow2$ kaonic transition. Choice (ii) represents a global fit[20] to all shift, width, and yield data over the Periodic Table. We will study the sensitivity of our calculated K^- capture results to the choice of $V^{K^-}_{opt}$ in Sec. IV. Here we wish to note that the difference between Rea for the two choices (i) and (ii) exceeds the error bars (omitted in the table) on each of these quantities; this is not the case for Ima, where the difference falls within the quoted[20] error bars.

The calculation of Eq. (44) implicitly assumed one orbit (n,L) of the K^- atom. This hypernuclear rate expression has to be averaged over the distribution $p(n,L)$ involved in the K^- capture process. Since Eq. (44) is independent

TABLE V. K^- optical-potential effective scattering length [Eq. (48)] and calculated shifts (negative for repulsion) and widths for the $3d\rightarrow2p$ transition in ^{12}C. The nuclear density (Ref. 21) used in these calculations is of type 3pF, with parameters $R=2.355$ fm, $a=0.5524$ fm, and $w=-0.149$.

K^- optical potential	a (fm)	ϵ_{2p} (keV)	Γ_{2p} (keV)	Γ_{3d} (eV)	Ref.
(i)	$0.45+i0.72$	-0.584	1.652	0.66	20
(ii)	$0.31+i0.79$	-0.582	1.489	0.62	20
Expt.		-0.590 ± 0.080	1.730 ± 0.150	0.98 ± 0.19	24

of the normalization of R_{nL} which appears quadratically in both numerator and denominator, and since the various R_{nL} for a given L are, to an excellent approximation, proportional to each other *in the nucleus* (note that the R_{nL} always appear multiplied by nuclear wave functions), the dependence of the calculated hypernuclear rate on n becomes (to better than 1%) redundant.[9] Hence, for a given L, we may calculate expression (44) with n arbitrarily chosen, subsequently averaging over the L distribution $P(L) = \sum_n p(n,L)$. A cascade calculation[23] which fits the absolute and relative x-ray intensities[24] in $K^- {}^{12}C$ yields

$$P(L=0)=0.7\%, \quad P(L=1)=17.8\%, \quad P(L=2)=81.5\%.$$
(49)

We shall neglect the s capture rate in this work (see, however, the discussion in the last paragraph of Sec. V B), effectively using 18% for capture from atomic p orbits and 82% from d orbits. Although we shall explore the $2p$ and $3d$ atomic wave functions below, we stress that the relatively sizable contributions from these orbits, $p(2p)=4.6\%$ and $p(3d)=47.9\%$, are far from saturating the capture process.

Previous calculations[4,9,14] of hypernuclear production in ${}^{12}C$ explicitly assumed capture from d orbits; capture from p orbits, which we find non-negligible and of intriguing consequences, was altogether ignored, while Ref. 9 also considered capture from s orbits, which they thought to constitute a sizable fraction of all K^- captures. For other targets in the p shell, capture from p orbits dominates at the beginning (Li), while the distribution (49) gives a fair representation at the end of the shell. Thus, for $K^- {}^{16}O$, Batty[23] reports

$$P(L=0)=(2\pm1)\%, \quad P(L=1)=(17\pm2)\% ,$$
$$P(L=2)=(79\pm3)\%, \quad P(L=3)=(1\pm1)\% .$$
(50)

Here the last observed x-ray transition is $4f \rightarrow 3d$, and capture from the $3d$ orbit is still the dominant one (25.0%) among d orbits, while the $2p$ orbit is found to contribute insignificantly (1.3%); in fact, the strongest p capture is now calculated to occur from $n=18$ (3.2%). The error estimates in Eq. (50) reflect variations in the capture rates which do not spoil the degree of fit to the x-ray data. Our calculation for ${}^{16}_\Lambda O$ employed K^- atomic wave functions generated from choice (i) of the K^- potential (Table V), with a 3pF nuclear density[21] specified by

$$R=2.608 \text{ fm}, \quad a=0.513 \text{ fm}, \quad w=-0.051 .$$

Graphic illustrations of the $3d$ and $2p$ $K^- {}^{12}C$ wave

functions in the nucleus are deferred to subsections C and D in connection with observations made there. These wave functions, particularly the $2p$ wave function, are essentially different from the r^L approximations devised earlier,[9] and the capture rates calculated here are correspondingly different.

B. Baryon wave functions

The radial wave functions $u_{n_B l_B j_B}(r)$ for nucleons and hyperons in a nucleus or hypernucleus, respectively, of atomic number A were generated by solving the Schrödinger equation with a real Woods-Saxon potential

$$V(r) = \frac{-V_0}{1+\exp[(r-R)/a]}, \quad R=r_0 A^{1/3} .$$
(51)

The geometry was fixed by setting $r_0=1.25$ fm and $a=0.6$ fm. The depth V_0 was adjusted for each partial wave to yield binding energies B as prescribed in Table VI. The Coulomb potential due to the nuclear-core charge distribution was included. The omission of a spin-orbit potential was compensated for by employing correspondingly different values of V_0 for spin-orbit doublet levels. The nucleon wave functions thus obtained were used in the construction of the DWIA integrals (38), and also in constructing the total nuclear density (47) which enters the "denominator" (46). Yet, for the construction of the latter quantity we checked other prescriptions as well, such as insisting that $\rho_N(r)$ reproduces in shape the nuclear charge distribution, or be derived from it by unfolding the proton size so as to obtain a possible point-nucleon distribution. The sensitivity of the calculated "denominator" (46) to variations in $\rho_N(r)$ can be estimated[20] to be about 15% when switching from charge distribution to point-nucleon distribution.

As for the hyperons, the $1p$ wave functions are of particular interest since the corresponding levels in ${}^{12}_\Lambda C$ are almost Λ unstable, and are well in the Σ^- continuum for ${}^{12}_\Sigma Be$. We verified that the dependence of the calculated rates on the (small) B_Y assumed was very moderate. Thus changing $B_\Lambda({}^{12}_\Lambda C)$ from 0.1 to 0.5 MeV brought modifications of a few percent at most. The value $B_{\Sigma^-}=0.5$ MeV used in the Σ-hypernuclear calculation was therefore chosen as a representative one. We checked that, by increasing it as much as to $B_{\Sigma^-}=5$ MeV, as used in Refs. 4 and 14, the 0^+ rate went up 5% and the 2^+ rate up 18%.

Because the baryon radial wave functions employed in the present work are real and nodeless, the calculated rates change smoothly and relatively slightly when these wave functions are varied within reasonable limits.

TABLE VI. Baryon binding energies B, in MeV, used to construct nucleon and hyperon wave functions in ${}^{12}C$ and ${}^{16}O$.

Orbit	$B(A=12)$				$B(A=16)$	
	p	n	Λ	Σ^-	n	Λ
$1s$	34.1	37.2	11.4	5	38.0	
$1p_{3/2}$	16.0	18.7	0.1	0.5	21.7	2.5
$1p_{1/2}$			0.1	0.5	15.7	2.5

TABLE VII. Pion optical-potential (opt. pot.) parameters [Eq. (52)] in pion-mass μ units and χ^2 per degree of freedom for fits (Ref. 27) to elastic scattering data on ^{12}C [A,B,C and (a),(b),(c)] and ^{16}O [(d)].

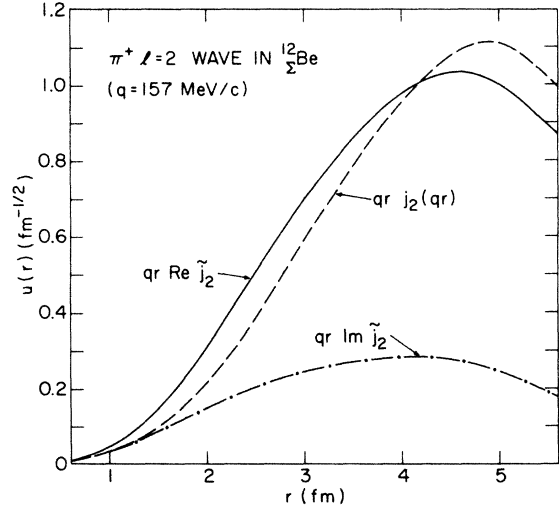| $T_L(\pi)$ (MeV)	π-^{12}C opt. pot.	b_0 (μ^{-1}) Re	Im	B_0 (μ^{-4}) Re	Im	c_0 (μ^{-3}) Re	Im	C_0 (μ^{-6}) Re	Im	ξ	$\dfrac{\chi^2}{df}$	Expt. Ref.
65	A	0.029	0	-0.165	0.014	0.217	0.020	-0.048	0.068	1.4	6.5	28
65	B	0.040	0	-0.200	0.014	0.266	0.026	-0.198	0.068	1.4	2.5	28
80	C	0.098	0	-0.312	0.014	0.227	0.017	-0.165	0.068	1.4	1.7	28
162	(a)	0.042	-0.63	0	0	0.042	0.362	0	0	1.4	7.0	29
162	(b)	0.268	0	0	0	0.036	0.206	0	-0.203	1.4	4.6	29
162	(c)	0.010	0.437	0	0	0.047	0.222	0	0	0	5.6	29
163	(d)	-0.112	0.348	0	0	0.194	0.121	0	0	0	3.8	30

FIG. 3. The $l=2$ π^+ distorted wave $u(r)=qr\tilde{j}_2(r)$, generated from parameter set A (Table VII), appropriate to the production of $^{12}_{\Sigma}$Be*(0⁺) in K⁻ capture from atomic d orbits in ^{12}C. The free wave $qrj_2(qr)$ is shown for comparison by the dashed curve.
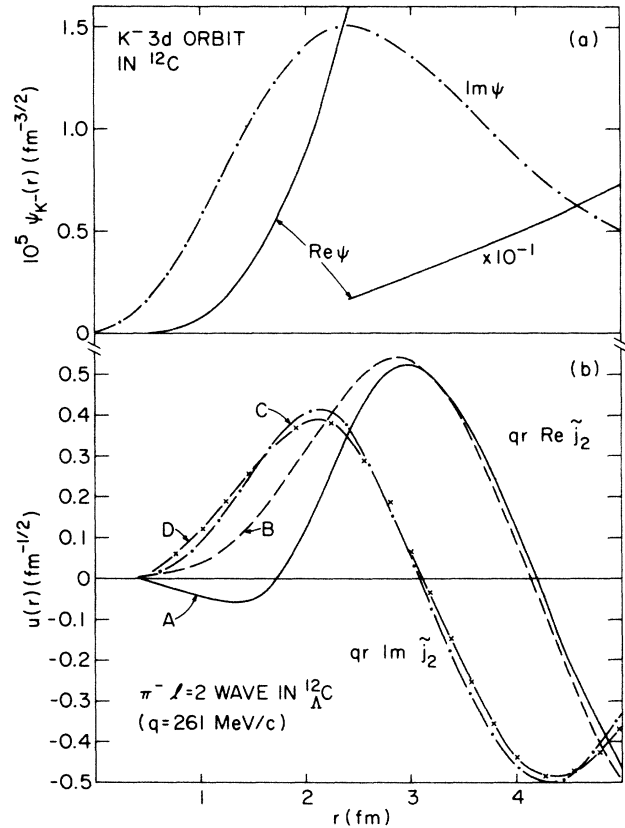
FIG. 4. (a) The K⁻ atomic $3d$ wave function $\psi_{K^-}(r)$ generated by the optical potential (i) (Table V), and (b) the $l=2$ π^- distorted wave $u(r)=qr\tilde{j}_2(r)$ generated from parameter sets (a) and (b) (Table VII) in ^{12}C. Curves A and B stand for Re$u(r)$ corresponding to sets (a) and (b), and curves C and D stand for Im$u(r)$, respectively. These K⁻ wave functions and π^- distorted waves are appropriate to the DWIA calculation of $^{12}_{\Lambda}$C*(0⁺) production in K⁻ capture from atomic d orbits in ^{12}C.

C. Pion distortion

The pion optical potential for scattering off isoscalar targets is taken to be of the form

$$2\mu V_{\text{opt}}^{\pi}(r) = -4\pi[(1+\mu/m)b_0\rho(r)+(1+\mu/2m)B_0\rho^2(r)]$$

$$+\nabla\cdot\frac{4\pi[(1+\mu/m)^{-1}c_0\rho(r)+(1+\mu/2m)^{-1}C_0\rho^2(r)]}{1+(4\pi/3)\xi[(1+\mu/m)^{-1}c_0\rho(r)+(1+\mu/2m)^{-1}C_0\rho^2(r)]}\nabla , \tag{52}$$

familiar from pionic-atom analyses[25] and low-energy pion scattering[26] ($T_\pi \lesssim 50$ MeV). This form has been recently studied by Friedman[27] for medium-energy pion-nuclear scattering by fitting the energy-dependent coefficients b_0, c_0, B_0, C_0, and ξ to elastic scattering differential cross sections. Although pions produced in K^- capture from rest scatter off the final hypernucleus, not in the isoscalar target nucleus, we have ignored the necessary correction terms simply because of ignorance. The pion optical potential (52) is inserted into the Klein-Gordon equation, with the appropriate π-hypernucleus kinematics, together with the Coulomb potential due to the finite charge distribution of the target nucleus to yield the partial-wave scattering solutions[22] $\tilde{j}_l(r)$. For Σ^- hypernuclear production in ^{12}C, we used a fractional charge $\frac{2}{3}$ for the outgoing π^+ in order to approximate the Coulomb potential due to the hypernucleus. Yet, the overall effect of the Coulomb potential on the pion partial waves, and subsequently on the calculated K^- capture rates, was found to be negligible for the low partial waves of interest here. The nuclear density is assumed to follow the shape of the point-nucleon distribution.

The parameters of the pion optical potentials used in this work, as fitted[27] to $\pi^{\pm}$ scattering data,[28-30] are given in Table VII together with the values of χ^2 per degree of freedom marking the quality of the fit.

In the Σ hypernuclear region, although the optical-potential parameters at the corresponding energies $T_L = 65$ and 80 MeV are required to evolve smoothly from those at lower energies[25,26] (e.g., by holding fixed some of the parameters: $\text{Im}b_0$, $\text{Im}B_0$, $\text{Im}C_0$, and ξ), the fit to the data is by no means unique, as shown by the existence of two solutions for $T_L(\pi)=65$ MeV. Parameter set A, in spite of the higher χ^2 value, fits the total reaction cross section better and, therefore, may as well be considered the favorable one.[27] A *global* measure of pion distortion is given by the ratio

$$D_L(q) = \frac{\int \rho_N(r)|R_{nL}(r)|^2|\chi_q(r)|^2 d^3r}{\int \rho_N(r)|R_{nL}(r)|^2 d^3r} , \tag{53}$$

tabulated in Table VIII, which gives the damping of the outgoing pion wave weighted by the process of K^- capture from rest. One naively expects D_L to be smaller than unity, but this need not be the case. The values calculated for fit A at $T_L(\pi)=72$ MeV ($q=156$ MeV/c) and shown in the table are about 1.1, and the sensitivity to the fit is rather small: D_2 changes from 1.099 to 1.114 in replacing fit A by C. For *specific* DWIA amplitudes, the situation is more involved. For example if we study the 0^+ excitation rate in $^{12}_\Sigma$Be for K^- capture from d orbits [cf. Eq. (49)], the only amplitude effective is $I^{(2)}_{1p,1p}$; considering for simplicity a point-Coulomb K^- wave function, the square of this amplitude $N^{(0)}_{1p,1p} = |I^{(2)}_{1p,1p}|^2$, is actually *larger* in the DWIA by about 30% than that for the PWIA at $q=156$ MeV/c, and this enhancement persists upon introducing a realistic K^- wave function into the calculation. The pion distorted wave $\tilde{j}_2(r)$ corresponding to this situation is shown in Fig. 3. Its real part is similar to the free wave $j_2(qr)$ both in shape and magnitude. The real part of $I^{(2)}_{1p,1p}$, therefore, is about the same as for free pions, while the smaller imaginary part adds incoherently. The DWIA result for $l=2$ is enhancement, but for the analogous case of capture from p orbits the 0^+ DWIA amplitude squared $N^{(0)}_{1p,1p} = |I^{(1)}_{1p,1p}|^2$ is somewhat suppressed, by 10% for a K^- point-Coulomb wave function and by 22% for a realistic wave function, relative to that for free pions. Here one recovers the naively expected notion that pion distortion causes a suppression of the calculated rates. Altogether, pion distortion effects do not play a significant role in K^- capture from rest to the Σ hypernuclear region.

The situation regarding pion distortion effects in K^- capture from rest to the Λ hypernuclear region is radically different. Looking at the entries in Table VII corresponding to this region [$T_L(\pi)=162$ MeV for ^{12}C], one notices that the p-wave parameters obtained are largely imaginary, which reflects the proximity to the 3,3 resonance. All three fits for this energy reproduce the measured[31] π^--^{12}C reaction cross section, 442±26 mb. The associated damping factors D_L in Table VIII are well below unity, as expected. For $^{16}_\Lambda$O, although only one genuine fit[27]

TABLE VIII. Values of $D_L(q)$ [Eq. (53)] for K^- capture from atomic orbit L to $^{12}_\Sigma$Be* states (set A), $^{12}_\Lambda$C* states [sets (a), (b), and (c)], and $^{16}_\Lambda$O* states [sets (c') and (d)]. The lab kinetic energies of the pion are given in parentheses in MeV.

| | | | $D_L(q)$ | | | |
| | A | (a) | (b) | (c) | (c') | (d) |
L	(72)		(162.7)		(167.9)	
1	1.140	0.449	0.499	0.302	0.286	0.360
2	1.099	0.541	0.574	0.414	0.376	0.455

[(d)] to the π^--^{16}O elastic scattering data[30] is shown in Table VII, we generated other ^{16}O optical potentials by rescaling the density $\rho(r)$ in the fits (a), (b), and (c) for ^{12}C, calling these modified sets (a'), (b'), and (c'), respectively.

The $l=2$ π^- distorted wave in ^{12}C at $T_L(\pi)=162.7$ MeV, corresponding to $q=261.1$ MeV/c, where $^{12}_\Lambda$C* 0$^+$ and 2$^+$ states are produced in K$^-$ capture from rest,[3,8,12] is shown in Fig. 4(b) for optical-potential parameter sets (a) and (b) of Table VII. In contrast to Fig. 3, appropriate to the Σ-hypernuclear excitation region, the imaginary part of $\tilde{j}_2(r)$ is appreciable, clearly indicating a strong absorption. The difference between sets (a) and (b) for Im$\tilde{j}_2$ is small (curves C and D, respectively). However, this difference for Re$\tilde{j}_2$ (A and B, respectively) is appreciable in the nucleus ($r \lesssim 3$ fm) and gives rise to a sensitivity of the calculated rates (particularly for the 0$^+$ excitation) to the pion-distortion parameter set employed. This sensitivity is likely to be enhanced when K$^-$ realistic wave functions are used, such as the one depicted in Fig. 4(a), because of interference induced by the imaginary parts of the wave functions. For the $L=2$ kaon and $l=2$ pion wave functions shown in Fig. 4, this is a pronounced but not dramatic effect, because although the imaginary parts are about the same size as the real parts in the surface region ($2 \lesssim r \lesssim 3$ fm), the kaon wave function is dominated by its real part at large distances ($4 \lesssim r \lesssim 5$ fm), which contribute significantly to the capture process. At such distances, the pion waves are fairly well reproduced [cf. Fig. 4(b)] by the strong-absorption limit

$$\tilde{j}_l(r) \underset{r \gtrsim R}{\sim} \tfrac{1}{2}[j_l(qr) - i n_l(qr)], \quad l \lesssim qR . \tag{54}$$

A consequence of this approximation is that the pion damping factor D_L, Eq. (53), appropriate to the global description of K$^-$ capture from rest, assumes values about 0.5 or less. This is confirmed by the values compiled in Table VIII. Of course, the DWIA suppression of specific rates could be much larger than the factor of 2—3 implied by the table and, indeed, this is the case for K$^-$ capture from rest to the Λ hypernuclear region (Sec. IV B).

D. Maximal DWIA suppression

The combination of a *realistic* K$^-$ atomic wave function with pion *distorted* waves leads to a remarkable suppression, between 2—3 orders of magnitude, of the PWIA rate for K$^-$ capture from p orbits to $^{12}_\Lambda$C*(0$^+$) and $^{16}_\Lambda$O*(0$^+$). In comparison, the DWIA suppression when a point-Coulomb K$^-$ wave function is used in the calculation is "only" about 1 order of magnitude. To gain insight into what happens here, we show in Fig. 5(a) the K$^-$ $2p$ atomic radial wave function (here denoted) $\psi(r)$ and in Fig. 5(b) the π^- $l=1$ distorted wave $u(r)=qr\tilde{j}_1(r)$ appropriate to $^{12}_\Lambda$C*(0$^+$) production. Both these wave functions enter the calculation of the *single* DWIA amplitude $I^{(1)}_{1p,1p}$ corresponding to 0$^+$ excitation; other J^π excitations in K$^-$ capture from p orbits receive contributions from DWIA amplitudes with higher values of l, $l=2,3$ for $J^\pi=1^-,2^+$, respectively, and the corresponding pion dis-

torted waves do not interfere as destructively with the K$^-$ $L=1$ wave function.

The vanishing of Reψ within the nucleus ($r \simeq 2.2$ fm) signals the existence of a K$^-$-^{12}C bound state due to the corresponding optical potential. The node of Reψ is required by the orthogonality of all $L=1$ K$^-$ *atomic* wave functions to the wave function of the K$^-$-nuclear state (which is too wide to be observed). *All* $L=1$ atomic wave functions, therefore, are very far from displaying the perturbative centrifugal behavior r^L sometimes assumed[9] within the nucleus. The origin of the suppression calculated for the 0$^+$ transition rate is now traced to the behavior of the product $u\psi$ in the region $r \lesssim 5$ fm. As for Re$(u\psi)$, it is remarkably small because Reψ vanishes where Re(u) peaks, just on the ^{12}C surface, and Imu vanishes where Imψ peaks there. As for Im$(u\psi)$, (Reψ)×(Imu) > 0 both inside and just outside the nucleus, while (Imψ)×(Reu) < 0 at the surface where both components are maximal; this forms a strong pattern of cancellations for Im$(u\psi)$. Therefore, the contribution to $u\psi$ from within the nucleus, only slightly important otherwise, becomes relatively significant—a feature that magni-
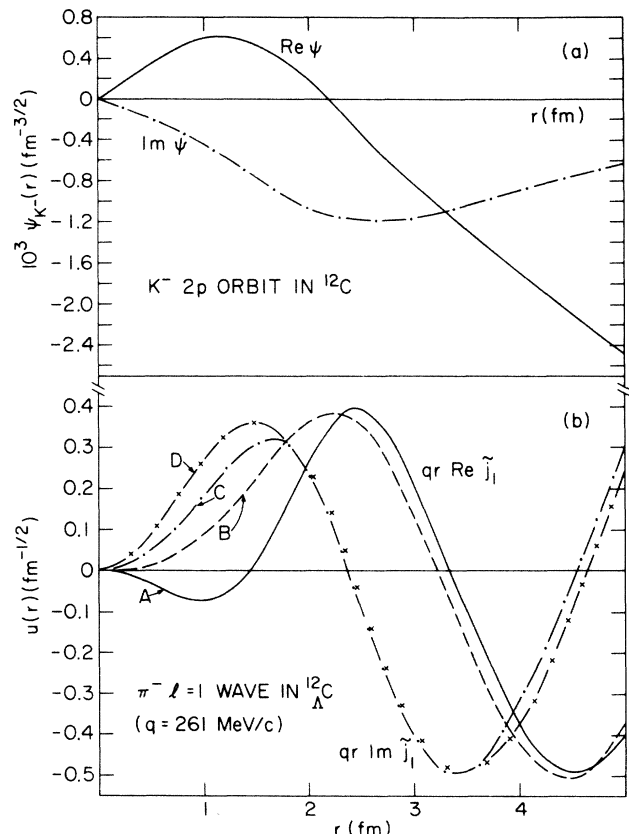
FIG. 5. (a) The K$^-$ atomic $2p$ wave function $\psi_{K^-}(r)$ generated by the optical potential (i) (Table V), and (b) the $l=1$ π^- distorted wave $u(r)=qr\tilde{j}_1(r)$ generated from parameter sets (a) and (b) (Table VII) in ^{12}C. Curves A and B stand for Re$u(r)$ corresponding to sets (a) and (b), and curves C and D stand for Im$u(r)$, respectively. These K$^-$ wave functions and π^- distorted waves are appropriate to the DWIA calculation of $^{12}_\Lambda$C*(0$^+$) production in K$^-$ capture from atomic p orbits in ^{12}C.

TABLE IX. Calculated K^- capture rates per Σ^- (in units of 10^{-2}) from d and p atomic orbits in ^{12}C to the summed $1p \to 1p$ 0^+ and 2^+ excitations in $^{12}_\Sigma$Be and the summed $1p \to 1s$ 1^- excitation and the summed $1p \to 1s$ 1^- excitations observed (Ref. 1). The pion-distortion parameter set used is C, except for $q=156$ MeV/c [$T_L(\pi)=72$ MeV], where both sets A and C are compared to each other. The K^- atomic wave functions were generated from optical potential (i). "Average" stands for 82% of d and 18% of p.

| | R/Σ^- (10^{-2}) | | | | | | | | | | | |
| | $q=173$ MeV/c C | | | $q=163$ MeV/c C | | | $q=156$ MeV/c C | | | A | | |
$J^\pi(^{12}_\Sigma\mathrm{Be})$	d	p	Average	d	p	Average	d	p	Average	d	p	Average
1^-	2.53	2.77	2.57									
0^+				4.76	3.49	4.53	4.91	4.10	4.76	4.78	4.07	4.65
2^+				3.25	3.94	3.37	3.45	4.28	3.60	3.48	4.23	3.61

fies, of course, the sensitivity of the calculation to details of the pion distortion [e.g., the difference between versions A and B of Reu (r) for $r \leq 1.8$ fm in Fig. 5(b)]. Furthermore, contributions from distances as large as 7 fm for ^{12}C are vital for convergence of the calculated DWIA integral.

IV. RESULTS OF THE CALCULATION

In this section we report the results of DWIA calculations for the rates per hyperon, using Eq. (44), for K^- capture from atomic p and d orbits in ^{12}C to Σ and Λ hypernuclear excitations. Some results are also given for ^{16}O. The input K^- atomic wave functions, the pion distorted waves, and the baryon bound-state wave functions were taken from Sec. III.

A. $^{12}_\Sigma$Be

The calculated K^- capture rates in ^{12}C per Σ^-, for the summed $1p(\mathrm{p}) \to 1p(\Sigma^-)$ 0^+ and 2^+ excitations and for the summed $1p(\mathrm{p}) \to 1s(\Sigma^-)$ 1^- excitations in $^{12}_\Sigma$Be, are given in Table IX in units of 10^{-2}. The K^- atomic wave functions were generated from the kaon optical potential (i) of Table V and the "average" stands for a weighted average of the calculated rates, 82% for capture from d orbits and 18% from p orbits. Using the kaon optical potential (ii) hardly changed the results. The dependence of the results on the pion distortion is weak, as can be seen by comparing the rates for $q=156$ MeV/c [$T_L(\pi)=72$ MeV] calculated with both parameter sets A and C of Table VII. Below, we also compare parameter sets A and B. The rates calculated for capture from p orbits are similar to those calculated for capture from d orbits which minimizes, of course, the sensitivity to the particular weighted average applied. For the wave function of the Σ^-, a binding energy of 5 MeV was assumed for the $1s$ state and 0.5 MeV for the $1p$ state. Varying these bindings within reasonable limits led to negligible changes in the calculated rates, of the order of several percent. Even if the $1p$ binding is increased to 5 MeV, as in Refs. 4 and 14, the calculated rates increase only by up to 10%. Of course, the lingering question of which wave functions are appropriate to the description of the observed $^{12}_\Sigma$Be peaks in the Σ^- continuum is not addressed by allowing for these variations.

In Tables X and XI we explore the sensitivity of the calculated $^{12}_\Sigma$Be* production rates to changing the pion optical potential (sets A and B of Table VII) and the K^- optical potential [(i) and (ii) of Table V]. The depicted results for $q=156$ MeV/c [$T_L(\pi)=72$ MeV] are normalized relative to those shown in Table IX for set A of pion-distortion parameters. We recall that set B fits the same pion scattering data. These tables show that switching from (i) to (ii) changes the $L=2$ rates by no more than 4% and the $L=1$ rates by no more than 10%, whereas switching from point-Coulomb wave functions to those due to either potential (i) or (ii) causes a decrease of the $L=2$ rates by up to 20% and the $L=1$ up to 40%; varying the pion distortion changes the rates calculated for capture from d orbits only by 1%, and rates for cap-

TABLE X. Sensitivity of calculated K^- capture rates per Σ^- from atomic d orbits in ^{12}C to the 0^+ and 2^+ summed excitations in $^{12}_\Sigma Be$ to the K^- atomic wave function (w.f.) and to the pion distortion used. The calculation used $q = 156$ MeV/c and all the rates were normalized relative to those for K^- optical potential (i) and pion-distortion parameter set A in Table IX.

| | K^- | R/Σ^- | | |
$J^\pi(^{12}_\Sigma Be)$	w.f.	Free	A	B
0^+	point Coulomb	0.904	1.179	1.170
	(i)	0.785	1[a]	0.989
	(ii)	0.826	1.037	1.026
2^+	point Coulomb	1.015	1.205	1.195
	(i)	0.984	1[b]	0.992
	(ii)	0.980	1.016	1.007

[a] Equivalent to a rate 4.780×10^{-2} per Σ^-.
[b] Equivalent to a rate 3.480×10^{-2} per Σ^-.

ture from p orbits by 4% or less. The overall effect of pion distortion, by comparing rates calculated with pion distortion included to rates with free pions, both with the same kaon wave function, is bounded by 30% for d orbits and by 40% for p orbits. However, one marked difference between the results for $L = 2$ and those for $L = 1$ is that while the rates for $L = 1$ in the columns headed "A" or "B" are smaller than the corresponding ones in the column headed "free," as expected due to the loss of pion flux to channels other than elastic scattering, this is not the case for $L = 2$. The $L = 2$ rates with free pions are *smaller* than those with pion distortion for both the 0^+ and 2^+ excitations (but not for the 1^- excitation, not considered in these tables). We have already discussed this feature, for the 0^+ $^{12}_\Sigma Be^*$ rates, in Sec. III C above.

Finally, in Table XII we give calculated production rates per Σ^- (in 10^{-2} units) for various types of excitations that are likely as well as unlikely [e.g., the (p^{-1},s) ground-state excitation] to explain the peak observed[1,8] at $q = 152$ MeV/c in the $^{12}_\Sigma Be$ spectrum. This table offers a comprehensive comparative listing of K^- capture rates in ^{12}C, beyond the few transitions discussed in detail in the preceding paragraphs. Our main interest, as discussed in Sec. V below, is in gauging the strength of the $1p_{3/2}(p) \rightarrow 1d_{5/2}(\Sigma^-)$ 1^- and 3^- transitions. All the rates in Table XII are given by the generic expression

$$\frac{R_{l_j \rightarrow l'_{j'}}}{\Sigma^-} = \frac{g(l_j, l'_{j'}) N^{(J)}_{l',l}}{\int \rho_p(r) |R_L(r)|^2 d^3r} , \quad (55)$$

where $\rho_p(r)$ is the ^{12}C proton density distribution normalized to 6, and $g(l_j, l'_{j'})$ is obtained from the appropriate coefficient of $N^{(J)}_{l',l}$ in Table III by multiplying by $2j + 1$. Expression (44) for the 0^+, 1^-, and 2^+ rates due to transitions originating from the $p_{3/2}$ protons in ^{12}C is a special case of Eq. (55). The capture rates listed in Table XII for transitions to the $d_{5/2}$ Σ^- shell are substantial, particularly the 1^- transition. We discuss the possible consequences in Sec. V A below.

B. $^{12}_\Lambda C$

The calculated K^- capture rates in ^{12}C per Λ, for the summed $1p(n) \rightarrow 1p(\Lambda)$ 0^+ and 2^+ excitations, and for the summed $1p(n) \rightarrow 1s(\Lambda)$ 1^- excitations in $^{12}_\Lambda C$, are given in Table XIII in units of 10^{-3}. In this DWIA calculation, the K^- atomic wave functions for d ($L = 2$) and p ($L = 1$) orbits were generated from the K^- optical potential (i), Table V. A weighted average of 82% for the former and 18% for the latter defines the entries marked "average." Rates are depicted for pions distorted by optical potentials (a)—(c) of Table VII. The momentum of the outgoing pion was set to $q = 261$ MeV/c for the $0^+, 2^+$

TABLE XI. Same as for Table X, but for captures from atomic p orbits.

| | K^- | R/Σ^- | | |
$J^\pi(^{12}_\Sigma Be)$	w.f.	Free	A	B
0^+	point Coulomb	1.783	1.615	1.554
	(i)	1.290	1[a]	0.958
	(ii)	1.408	1.079	1.036
2^+	point Coulomb	1.583	1.533	1.495
	(i)	1.173	1[b]	0.972
	(ii)	1.299	1.104	1.078

[a] Equivalent to a rate 4.071×10^{-2} per Σ^-.
[b] Equivalent to a rate 4.226×10^{-2} per Σ^-.

TABLE XII. Calculated K^- capture rates per Σ^- (in units of 10^{-2}) from d and p atomic orbits in ^{12}C to various excitations in $^{12}_{\Sigma}Be$. The pion momentum $q = 152$ MeV/c corresponds to the third peak reported in Ref. 8. The K^- atomic wave functions were generated from optical potential (i), and the pion-distortion parameter set A was used. "Average" stands for 82% of d and 18% of p. The $1d$ Σ^- wave functions correspond to assumed binding of 0.5 MeV.

$^{12}_{\Sigma}Be$		R/Σ^- (10^{-2})		
		d	p	Average
(p^{-1},s)	1^-	3.23	3.42	3.26
$(p_{3/2}^{-1},p)$	0^+	4.80	4.46	4.74
	2^+	3.64	4.45	3.79
(s^{-1},s)	0^+	0.85	2.15	1.08
$(p_{3/2}^{-1},d_{5/2})$	1^-	6.02	5.48	5.92
	3^-	2.41	1.83	2.31
$(p_{3/2}^{-1},d_{3/2})$	1^-	0.67	0.61	0.66
	3^-	3.62	2.75	3.46

excitations and 273 MeV/c for the 1^- ground state. The DWIA rates for capture from p orbits are generally smaller, particularly for 0^+, than those for d orbits. This is just the opposite of the trend of the PWIA and is explained by the increased pion absorption triggered by the weaker centrifugal barrier for kaons of lower angular momentum L. For this reason, the "average" capture rates to states in $^{12}_{\Lambda}C$ are roughly determined by the rates calculated for capture from d orbits.

The main feature of the DWIA rates in Table XIII is their sensitivity to the employed pion optical potential. This allows for as large variation as a factor of 3 in the calculated "average" rates for the 0^+ excitations and about 50% for the other rates. The variation would have been considerably larger, if the calculated rates were dominated by K^- captures from p orbits, with a variation of the calculated 0^+ rate spanning, then, 2 *orders of magnitude*. The origin of this spectacular sensitivity is traced back to the pattern of cancellations discussed in Sec. III D.

In Tables XIV and XV we compare rates calculated with pion DW's to those calculated with pion PW's, and study the dependence of the calculated rates, for PW's as well as for each of the three sets of pion distortion, on the K^- atomic wave function: point Coulomb (essentially

r^L) and those due to K^- optical potentials (i) and (ii). The rates in these tables were normalized to those for K^- wave function (i) and pion distortion (a). A value $q = 255$ MeV/c for the pion momentum, differing somewhat from those used in Table XIII, was uniformly chosen for display in order to allow for as accurate comparison as possible with the eikonal-distortion calculation of Ref. 9 for capture from d orbits. By comparing the columns (a)—(c) for pion distortion with the column headed "free" in Tables XIV and XV, we deduce that the suppressive effects of using pion DW's on the capture rates are stronger for p orbits than for d orbits (already remarked above), and become increasingly larger with decreasing transition multipolarity, here identical with J, for capture from a given K^- orbit. The most suppression due to the use of the DWIA, therefore, occurs in the 0^+ rates calculated for capture from p orbits (1—3 orders of magnitude), but even for capture from d orbits this suppression is sizable (about 1 order of magnitude). The least suppression, by about a factor of 3, is found for the 2^+ rates in capture from d orbits.

While the dependence of the calculated rates on the K^- atomic wave function for PW pions is weak, their variations not exceeding 15%, the use of *realistic* K^- wave functions is essential for a precise evaluation of the Λ-hypernuclear production rates when distorted waves are used for the outgoing pion. For example, for 2^+ production, the least suppressed of all, the use of K^- wave function of type (i) or (ii) reduces the calculated rate by up to 35% for $L = 2$ and by up to 60% for $L = 1$, relative to the rate calculated with a point-Coulomb K^- wave function. This effect is particularly strong for 0^+ production in capture from $L = 1$, which also provides for the only case in these tables where a strong sensitivity to the type [(i) or (ii) here] of K^- realistic wave function was found; otherwise, the dependence of the calculated rates on which of the types (i) or (ii) is employed for the K^- wave function is well bounded within 20% variation.

The eikonal-distortion calculation of Ref. 9, with results shown in the last column of Table XIV, assumed r^2 $L = 2$ K^- wave functions and, therefore, can no longer be considered as a quantitative calculation, particularly since it misses quite badly in the suppression calculated here for the 0^+ rate. The small-angle approximation inherent in the eikonal calculation cannot be expected to work well for the pion low partial wave, $l = L$, encountered in the evaluation of this rate. Similar, but stronger conclusions hold for capture from $L < 2$ orbits.

TABLE XIII. Calculated K^- capture rates per Λ (in units of 10^{-3}) from d and p atomic orbits in ^{12}C to the summed $1p \rightarrow 1s$ 1^- excitation ($q = 273$ MeV/c) and the summed $1p \rightarrow 1p$ 0^+ and 2^+ excitations ($q = 261$ MeV/c) in $^{12}_{\Lambda}C$, for pion-distortion parameter sets (a)—(c). The K^- wave functions were generated from optical potential (i). "Average" stands for 82% of d and 18% of p.

$J^\pi(^{12}_{\Lambda}C)$	(a)			(b)			(c)		
	d	p	Average	d	p	Average	d	p	Average
1^-	2.38	0.74	2.08	3.41	2.27	3.21	2.06	1.34	1.93
0^+	0.92	0.01	0.76	1.97	0.10	1.64	2.55	0.82	2.24
2^+	7.46	4.17	6.87	9.03	6.11	8.51	6.30	3.70	5.83

TABLE XIV. Sensitivity of calculated K^- capture rates per Λ from atomic d orbits in ^{12}C to the 1^-, 0^+, and 2^+ summed excitations in $^{12}_\Lambda C$ to the K^- atomic wave function (w.f.) and to the pion distortion used. The calculation used $q = 255$ MeV/c and all the rates were normalized relative to those for K^- optical potential (i) and pion-distortion parameter set (a). The values in square brackets for *eikonal* stand for the eikonal distortion from Ref. 9.

$J^\pi(^{12}_\Lambda C)$	K^- w.f.	Free	R/Λ (a)	(b)	(c)	[eikonal]
1^-	point Coulomb	4.56	1.51	1.77	1.14	[1.63]
	(i)	5.09	1[a]	1.35	0.81	
	(ii)	4.61	0.98	1.29	0.79	
0^+	point Coulomb	17.8	2.25	3.38	3.87	[6.05]
	(i)	18.3	1[b]	2.15	2.52	
	(ii)	17.3	0.93	1.90	2.53	
2^+	point Coulomb	3.09	1.43	1.63	1.21	[1.25]
	(i)	2.97	1[c]	1.21	0.85	
	(ii)	2.99	1.06	1.26	0.91	

[a] Equivalent to a rate 3.13×10^{-3} per Λ.
[b] Equivalent to a rate 1.14×10^{-3} per Λ.
[c] Equivalent to a rate 7.81×10^{-3} per Λ.

C. $^{16}_\Lambda O$

Here we give results for the excitation of 0^+ and 2^+ states from the $1p_{1/2}$ neutron shell in ^{16}O to the $1p_{1/2}$ and $1p_{3/2}$ (almost degenerate) Λ subshells, respectively, in K^- capture from atomic orbits in ^{16}O. These excitations are stable to Λ emission and may have been observed[12] via the proton emission channel (3b) through the observation of a peak in the pion spectrum for pion kinetic energy $T_{\pi^-} \sim 163$ MeV. The rates per Λ are given by multiplying the corresponding entries in Table III by 2, the occupancy of the neutron $p_{1/2}$ subshell in ^{16}O. Thus,

$$R(0^+)/\Lambda = \frac{2N^{(0)}_{1,1}}{\int \rho_n(r)\,|R_L(r)|^2 d^3r},$$

$$R(2^+)/\Lambda = \frac{4N^{(2)}_{1,1}}{\int \rho_n(r)\,|R_L(r)|^2 d^3r}, \tag{56}$$

where we suppressed the dependence on j. Neglecting this dependence altogether, the rate for the other 0^+ excitation, due to the $1p_{3/2} \to 1p_{3/2}$ transition, is twice that given by Eq. (56) and the rates for the other 2^+ excitations, due to the $1p_{3/2} \to 1p_j$ transitions, are each identical with that given by Eq. (56). Retaining the j dependence through the known 6 MeV binding difference between the $p_{1/2}$ and $p_{3/2}$ neutrons in ^{16}O, we found differences about $10-15\%$ between the 2^+ rates for all pion distortions employed and deviations as large as 25% from the ratio 2 for the 0^+ rates when using pion distortion sets (a') and (b').

The results of interest are depicted in Table XVI in units of 10^{-3} for kaon wave function (i) and pion distortion sets (a')—(c') and (d). The latter set is listed in Table VII and is based on actually fitting the π^--^{16}O scattering data,[30] whereas the former sets have parameters identical to those of (a)—(c), respectively, for π^--^{12}C, except for rescaling the density. The rates shown in Table XVI bear

TABLE XV. Same as for Table XIV, but for captures from p orbits.

$J^\pi(^{12}_\Lambda C)$	K^- w.f.	Free	R/Λ (a)	(b)	(c)
1^-	point Coulomb	21.2	3.86	6.54	4.01
	(i)	19.8	1[a]	2.91	1.57
	(ii)	18.6	1.00	2.80	1.64
0^+	point Coulomb	1420	99	114	334
	(i)	1530	1[b]	13	95
	(ii)	1340	4.7	3.6	103
2^+	point Coulomb	6.97	2.42	2.82	1.87
	(i)	6.11	1[c]	1.43	0.86
	(ii)	6.24	1.19	1.61	1.01

[a] Equivalent to a rate 1.09×10^{-3} per Λ.
[b] Equivalent to a rate 0.01×10^{-3} per Λ.
[c] Equivalent to a rate 4.70×10^{-3} per Λ.

TABLE XVI. Calculated K^- capture rates per Λ (in units of 10^{-3}) from d and p atomic orbits in ^{16}O to the $1p_{1/2}\to1p$ 0^+ and 2^+ excitations ($q=268$ MeV/c) in $^{16}_\Lambda O$, for various pion-distortion parameter sets. The K^- wave functions were generated from optical potential (i). "Average" stands for 82% of d and 18% of p.

Pion distortion	K^- orbit	R/Λ (10^{-3})	
		0^+	2^+
free	d	6.76	7.84
	p	5.18	10.24
	average	6.48	8.27
(a')	d	0.107	1.57
	p	0.008	0.590
	average	0.089	1.39
(b')	d	0.298	2.11
	p	0.030	1.25
	average	0.250	1.96
(c')	d	0.556	1.28
	p	0.195	0.774
	average	0.491	1.19
(d)	d	0.474	1.47
	p	0.227	0.748
	average	0.430	1.34

similar trends to those for $^{12}_\Lambda C$ in that pion distortion effects are large, larger for the 0^+ rate (which is suppressed by over an order of magnitude) than for the 2^+ rate and the captures from p orbits are more suppressed by the pion distorted waves than the corresponding captures from d orbits. The cancellation discussed in Sec. III D for the 0^+ excitation in $^{12}_\Lambda C$ also persists here for the same parameter sets (a') and (b'). Set (d) gives capture rates similar to those calculated with set (c'). These latter two fits yield a moderate value for the ratio of rates $2^+/0^+$, 2.4—3.1, in contrast with 8—16 for the former two fits.

V. SUMMARY AND DISCUSSION

Our calculated "rates per hyperon," Eq. (22), were presented in Sec. IV for K^- capture from rest in ^{12}C to excitations in $^{12}_\Sigma Be$ and $^{12}_\Lambda C$, and in ^{16}O to excitations in $^{16}_\Lambda O$. These rates exhaust only one of the three factors that figure in Eq. (20) for "rates per stopped K^-," the other two being (i) $R(\pi^{-\tau-1/2}Y)$, the primary branching ratio for the particular pion-hyperon channel studied (see Table I), and (ii) the simple kinematic factor $q_f\omega_f/\bar{q}_f\bar{\omega}_f$ appropriate to a specific final state in that particular channel. Values of this latter factor are listed in Table XVII for several excitations in $^{12}_\Sigma Be$ and $^{12}_\Lambda C$. The values chosen for $\bar{q}_f$ were estimated from the observed spectra,[8] by identifying $\bar{q}_f$ with the quasifree peak pion momentum. We believe that the values for the kinematic factor arrived at in the table, which give rise to a 13—46% enhancement of the calculated rates, provide a conservative estimate of this factor: extrapolation of the quasifree formulation and fit given in Ref. 32 would lead to

TABLE XVII. Values of kinematic enhancement factor $(q_f\omega_f/\bar{q}_f\bar{\omega}_f)$ in K^- capture from rest in ^{12}C. The values of $\bar{q}_f$ were estimated from the spectra in Ref. 8 and the values of q_f represent the hyperon orbits as observed (Refs. 3, 8, and 12). Assignments or values in parentheses are uncertain.

Hyper-nucleus	$\bar{q}_f$ (MeV/c)	Hyperon orbit	q_f (MeV/c)	$q_f\omega_f/\bar{q}_f\bar{\omega}_f$
$^{12}_\Sigma Be$	140	$1s$	(173)	(1.386)
		$1p$	160	1.226
		$(1d)$	152	1.132
$^{12}_\Lambda C$	220	$1s$	273.2	1.456
		$1p$	261.1	1.345

$\bar{q}_f(^{12}_\Lambda C)\simeq225$ MeV/c, sufficiently close to the value $\bar{q}_f=220$ MeV/c used in the table.

In the subsections below we summarize the results of this paper for R_{if}/K^- and discuss them in relationship to the experiments[1,3,8,12] and calculations[4,9,14] published to date.

A. $A=12$ Σ hypernuclei

1. $^{12}_\Sigma Be$

The excitation spectrum[1] of this Σ^- hypernucleus shows a striking evidence for three peaks in the energy range 2—12 MeV in the Σ^- continuum, with widths of about 5 MeV each. The latest determination of the peak positions and their excitation rates per stopped K^- in $^{12}C(K^-,\pi^+)$ is due to Ref. 8 (Table 2). In Table XVIII here we list the pion momenta and capture rates corresponding to these peaks, together with our calculated rates. In transforming the reported[8] "intensity per $K^-\to\pi^+$ all" and the calculated "rates per Σ^-" from Table IX here, we multiplied by 0.136 for the primary branching ratio tabulated in Table I here to obtain "rates per K^-;" for the calculated rates, we also applied the kinematic enhancement factors from Table XVII.

The first two peaks, in descending order of $q(\pi^+)$, are generally believed[1,4,6,7] to be due to the transition $1p(p)\to1p(\Sigma^-)$. Therefore, the calculated rate assigned to these peaks was worked out from the 0^+ and 2^+ rates per Σ^- of Table IX, after averaging the results corre-

TABLE XVIII. Measured (Refs. 1 and 8) and calculated (present work) rates (in %) per stopped kaon in K^- $^{12}C\to\pi^+$ $^{12}_\Sigma Be$. The assignment $1d_{5/2}$ in the bottom line is tentative (Ref. 7).

$q(\pi^+)$ (MeV/c)	$(R/K^-)_{expt}$ (%)	$l_j(\Sigma^-)$	$J^\pi(^{12}_\Sigma Be)$	$(R/K^-)_{calc}$ (%)
?	?	$1s_{1/2}$	1^-	0.48
164.0±0.5	0.81±0.07	$1p$	0^++2^+	1.36
158.2±0.5	0.37±0.07			
152.5±0.5	0.38±0.07	$(1d_{5/2})$	1^-	0.65
			3^-	0.42

sponding to $q = 163$ and 156 MeV/c, both for set C of pion distortion. The summed $(0^+ + 2^+)$ calculated rate of 1.36% per K^- compares well with the sum $(1.18 \pm 0.10)\%$ reported for the two peaks. However, one must bear in mind that the $1p(\Sigma^-)$ configuration may exhibit a considerable fragmentation[11] to the extent that no more than 60–70% of its strength could be identified with distinct peaks in the data. Furthermore, although the calculated Σ^- rates were remarkably stable to the input K^- and π^- wave functions, as discussed in Secs. III C and IV A, there was (Sec. III B) about 15% uncertainty in the calculation due to allowed variations in the Σ^- wave function and the nuclear density. Finally, a necessary input to any spectroscopic study of the $1p(\Sigma^-)$ configuration in $^{12}_\Sigma$Be is the ratio of 2^+ to 0^+ rates which we find to be given by

$$2^+/0^+: \quad 0.75 \pm 0.05 , \tag{57}$$

where the error estimate follows an educated guess.

The interpretation of the third observed peak, for $q(\pi^+) = 152.5$ MeV/c, is unsettled yet. Assuming Σ-nuclear $p_{1/2}$-$p_{3/2}$ spin-orbit splitting between 3 and 5 MeV, it was possible to reproduce[7] the first two peaks, but no reasonable residual ΣN interaction was found able to displace a substantial $1p(p) \rightarrow 1p(\Sigma^-)$ strength to the region of the third peak. While this peak could, on the basis of energetics alone, belong to the $1d_{5/2}(\Sigma^-)$ configuration, it was acknowledged[7] that no compelling reason existed why $^{11}B \otimes 1d(\Sigma^-)$ states should be narrow and their excitation strength sufficiently unfragmented to yield a peak at such relatively high excitation (11 MeV in the Σ^- continuum). On the other hand, assuming the spin-orbit splitting to be close to 10 MeV, as favored in Ref. 6 so that the first and third peaks are essentially due to the $1p_{3/2}$ and $1p_{1/2}$ Σ^- configurations, respectively, the spectroscopic calculations[6,7] could not account for the second observed peak. Of course, if the spin-orbit splitting were as large as that, this peak might be tentatively assigned to the $1d_{5/2}(\Sigma^-)$ configuration. Because the intensities reported for the second and third peaks are identical to each other, the assumption that the rate observed for the $1p \rightarrow 1p$ transition is about 1.2% per K^- remains intact in either case, irrespective of whether the second or third observed peak is tentatively assigned to the $1d_{5/2}(\Sigma^-)$ configuration. This argumentation requires then a rate of about 0.4% per K^- to be provided by the theoretical calculation for the excitation of the $1d_{5/2}(\Sigma^-)$ state. Two possibilities are shown in the table: if the state thus excited is 1^-, its lack of fragmentation would point to a rather pure configuration, $^{11}B_{g.s.} \otimes 1d_{5/2}(\Sigma^-)$. The calculated rate per Σ^- given in Table XII under $(p_{3/2}^{-1}, d_{5/2})$ is to be multiplied by the Cohen-Kurath[33] spectroscopic factor 0.712 for $^{11}B_{g.s.}$ in $^{12}C_{g.s.}$, which together with the other multiplicative factors considered above give the value 0.65% listed in the table. On the other hand, if the excited state is 3^-, its observed rate of excitation could saturate as well the strength of $^{11}B(\frac{1}{2}^-;$ 2.12 MeV$) \otimes 1d_{5/2}$; we added this strength by multiplying the rate per Σ^- tabulated under $(p_{3/2}^{-1}, d_{5/2})$ by $\frac{5}{2}$, due to the different coefficient of $N_{2,1}^{(3)}$ for the transition

$p_{1/2} \rightarrow d_{5/2}$ in Table III, and then multiplying by the $^{11}B(\frac{1}{2}^-)$ spectroscopic factor[33] 0.188 (rather than by 0.712 for the ordinary $^{11}B_{g.s.}$ component). This procedure gave the value 0.42% listed in the table. Although this calculated 3^- rate agrees very well with the measured rate for exciting the second or third peak, we do not feel—in view of the crudeness of such estimates—that this rules out the 1^- excitation as a candidate for this peak. Preliminary calculations[11] show that the small-angle (K^-,π^+) reaction at 720 MeV/c (see Ref. 15) is capable of distinguishing between these two possibilities, since the 3^- rate in flight is considerably smaller than the 1^- rate which competes favorably with the dominant 0^+ $1p \rightarrow 1p$ transition rate.

An extremely interesting question is where the $^{12}_\Sigma$Be ground-state transition strength is located. The calculated $1s_{1/2}(\Sigma^-)$ 1^- rate for K^- capture from rest in ^{12}C, as given in Table XVIII, is sufficiently large to allow detection if the ground state is not wider than, say, 10 MeV. While K^- capture from rest provides, in principle, a favorable reaction to produce Σ-hypernuclear ground states on light targets, the present lack of experimental evidence[1,8] for the excitation of such ground states on ^{12}C is consistent with the failure to observe Σ-hypernuclear ground states in any of the experiments reported to date on light nuclei.

The only other calculation of K^- capture rates in ^{12}C into states of $^{12}_\Sigma$Be is due to Matsuyama and Yazaki.[4,14] A comparison between these results and those of the present work was given in a preliminary report.[16] The tabulation in Ref. 14 gives rates which are generally *a factor of 2* below our calculated rates. However, we have recently learned[34] that the calculation of Matsuyama and Yazaki, due to wrong consideration of the Σ-hypernuclear kinematics, was done for $q \sim 200$ MeV/c, not for $q \sim 160$ MeV/c as it should have. A preliminary check[34] into their output assured us that the factor of 2 discrepancy mentioned above was largely due to this oversight. We conclude, therefore, that the state of the art in calculating K^- capture rates into Σ-hypernuclear states is satisfactory.

2. $^{12}_\Sigma$C

Yamazaki *et al.* have recently presented[8] the π^- spectrum for K^- capture from rest in ^{12}C to the Σ-hypernuclear region. Again, three peaks were observed in the $^{12}_\Sigma$C continuum. However, since both $T = \frac{1}{2}$ and $\frac{3}{2}$ states are excited in the (K^-,π^-) reaction, whereas only the $T = \frac{3}{2}$ counterparts of these are excited in the (K^-,π^+) reaction discussed above, there is more room to accommodate the observed $^{12}_\Sigma$C levels within the $1p(\Sigma)$ configuration. The calculations of Refs. 7 and 11 find two main $T = \frac{3}{2}$ peaks [directly related to the two $1p(\Sigma^-)$ excitations discussed above], but perhaps only one distinct $T = \frac{1}{2}$ peak, because the residual ΣN interaction produces coherencies in the $T = \frac{1}{2}$ hypernuclear sector which tend to keep the (K^-,π^-) strength unfragmented. According to Eqs. (30) and (39) of Sec. II, one expects equal "rates per Σ" (irrespective of which charge state) in the $(K^-,\pi^\pm)$ reactions, if the *summed* $1p(\Sigma)$ configura-

tion is considered and charge-dependent (Coulomb and kinematic) factors are negligible in the production stage. The intensities presented in Ref. 8, in Table 2 there for (K^-,π^+) and Table 3 there for (K^-,π^-), are indeed roughly comparable to each other, although it was unclear to us whether these intensities were always derived from the raw data or that different cuts were applied through the derivation. For this reason we avoid further discussion of the $^{12}_\Sigma C$ spectrum, except to state that if summed rates per stopped K^- are ever derived, they should be larger than the corresponding $^{12}_\Sigma Be$ rates by the ratio of K^- absorption fractions (Table I): $(0.305 + 0.027)/ 0.136 = 2.44$. This observation follows from the discussion in Secs. II C and II D above.

B. $^{12}_\Lambda C$

The observed π^- spectrum[3,8] in the reaction $^{12}C(K^-,\pi^-)$ with stopped kaons gives evidence for two $^{12}_\Lambda C$ peaks which due to their energetics, and by comparison with in-flight measurements, are generally assigned to the $1s_\Lambda$ 1^- ground state $(q=273$ MeV/c) and to $1p_\Lambda$ 0^+ and 2^+ states $(q=261$ MeV/c). The recent reanalysis[12] of the emulsion data[13] resolved the latter peak into three components. In Table XIX we list the capture rates reported for these peaks, together with our calculated rates. As discussed in Sec. III C and IV B, the calculated Λ-hypernuclear rates are sensitive to the pion distortion entered into the calculation and, therefore, are presented in the table here for all three pion distortions, (a)—(c), used there. We emphasize again that all three give a fair fit to $\pi^- - {}^{12}C$ elastic scattering data and total reaction cross section.

The 1^- calculated rates increase by about 60% in going from sets (a) and (c) to set (b). However, the 50% error bars for the only reported[3] rate easily accommodate all these calculated values within a very reasonable agreement. A lesser degree of variation is noted between the rates calculated for the summed $1p(n) \rightarrow 1p(\Lambda)$ transition to 0^+ and 2^+ states, but the reported[3,8,12] rates vary over more than an order of magnitude. We feel that the rate $(0.3\pm0.1)\times10^{-3}$ quoted from Ref. 3 is an underestimate; if pion distortion effects were as large as to reduce the calculated rates by yet another factor of 2—3 beyond the almost order of magnitude suppression already undergone, there surely would arise higher DWIA corrections to partly restore these suppressed rates. On the other hand, we

also feel that the rate $(8\pm1)\times10^{-3}$ deduced from Table 4 of Ref. 8 (by multiplying either of the intensities given there by the appropriate *primary* branching ratio from Table 1 there, or Table I here) is an overestimate; it is implausible that the $1p(n) \rightarrow 1p(\Lambda)$ transition could exhaust as much as 10% of the overall direct Λ-hypernuclear production when the relatively large baryonic momentum transfer (here equal to $\bar{q}_f \sim 220$ MeV/c) allows for abundant continuum excitation.

However, we could be wrong in our interpretation of the rates reported by Yamazaki et al.,[8] in case these actually refer to intensities per the *observed* π^- spectrum.[35] This could result in a reduction of the value deduced in Table XIX for the rate per stopped K^- by, at most, a factor of 2, a resultant rate which still appears on the high side. Finally, the rate 1.2×10^{-3} reported in Ref. 12 should be corrected for loss of $^{11}_\Lambda B$ tracks in the emulsion work. The corrected rate is estimated[36] to be about 1.8×10^{-3}, which would leave our calculated rate short of reproducing the observed $1p \rightarrow 1p$ rate by a factor of 2. The uncertainty in the theoretical calculation for this summed rate is estimated as 30% due to sensitivity to the treatment of pion distortion and another 30% due to a possible systematic error in the determination of the primary branching ratio[17] for $K^-n \rightarrow \pi^-\Lambda$.

The uncertainty arising from pion distortion is maximal in our calculations for the ratio $2^+/0^+$ shown in the last column of Table XIX. Optical potential sets (a) and (c), which gave practically identical results for the summed $1s_\Lambda$ and the summed $1p_\Lambda$ transition rates, differ by as much as a factor of 4 for this ratio, while set (b) gives a value intermediate to both. In spite of this wide variation, all the calculations (including those in Refs. 9 and 14 mentioned below) gave values larger than unity, and this consensus is one of the main reasons for identifying[12] the narrower of the two overlapping peaks at $q(\pi^-)=261.1$ MeV/c with the main 0^+ state. If the broader of the two is assigned 0^+, the ratio $2^+/0^+$ derived from the observed spectrum becomes 0.74, as given in parentheses in the table.

A comparison between our calculated rates for $^{12}_\Lambda C$ and those due to Hüfner et al.[9] and Matsuyama and Yazaki[4,14] was given in a preliminary report.[16] To briefly repeat it, we mention that the calculation of Ref. 9 assumed essentially point Coulomb K^- wave functions and described pion distortion in the eikonal approximation. As shown in Table XIV, in Sec. IV B above and discussed there, these approximations tend to produce somewhat larger rates, particularly for the 0^+ excitation, for K^- capture from d orbits. Furthermore, Hüfner et al. did not consider captures from p orbits, which give intrinsically smaller Λ-hypernuclear rates because pion distortion is more effective in these captures. The result of these approximations is that the $^{12}_\Lambda C$ rates calculated in Ref. 9, for captures from d orbits, are about a factor of 2 higher than ours.

The calculation of Refs. 4 and 14 also gives rates about a factor of 2 higher than ours, which we believe is mainly due to the extra factor $D_L(q)$ [Eq. (53)] in their formulation, by which they divided the calculated "rates per hyperon." While this factor is close to unity for Σ-

TABLE XIX. Measured (Refs. 3, 8, and 12) and calculated (present work) rates (in 10^{-3}) per stopped K^- in the reaction $K^- {}^{12}C \rightarrow \pi^- {}^{12}_\Lambda C$.

| | R/K^- (10^{-3}) | | |
	$1s_{1/2}(1^-)$	$1p(0^+ + 2^+)$	$2^+/0^+$
Expt. (Ref. 3)	0.2±0.1	0.3±0.1	
Expt. (Ref. 8)		8 ±1	
Expt. (Ref. 12)		≥1.2	4.3 (0.74)
Theor. (a)	0.21	0.72	9.0
Theor. (b)	0.33	0.96	5.2
Theor. (c)	0.20	0.76	2.6

hypernuclear production, it is about 0.5 for Λ-hypernuclear production in K⁻ capture from d orbits (Table VIII here). As argued in Sec. II above, it is unjustified to keep track of the pion damping $|\chi_q(r)|^2$ in summing up the K⁻ capture events to obtain the right normalization for a specific rate per stopped K⁻; *all* kaons get captured when brought to rest, irrespective of whether the produced pion escaped from the final hypernucleus elastically, inelastically, or got absorbed. If, on the other hand, one sums up the π^- *emission* spectrum alone, not normalizing with respect to the total number of captures per stopped K⁻, pions due to both elastic as well as *inelastic* scattering should be included. But the pion damping $|\chi_q(r)|^2$ in the factor $D_L(q)$ leaves pion true absorption *and* inelastic scattering out of the corresponding summation, because it accounts for damping of anything but elastic scattering. For the pion energies met in the Λ-hypernuclear production region, pion inelastic and pion true-absorption cross sections are roughly comparable to each other.[31] Therefore, the procedure[4,14] of using $D_L(q)$ in relating calculated rates to experimentally reported rates is unjustified. Note that summing over the pion emission spectrum requires in first approximation to switch off the Imb_0, Imc_0 terms of V_{opt}^π, Eq. (52), which give the quasielastic part of its reactive content. Finally, we comment that the Λ-hypernuclear rates published in Refs. 4 and 14 apparently[34] were calculated for $q(\pi^-) \sim 290$ MeV/c, a substantially higher momentum than those corresponding to the $^{12}_\Lambda$C excitations of interest here.

Hüfner *et al.*[9] considered the possibility that a significant fraction of K⁻ captures in ^{12}C occur from $s(L=0)$ orbits, and found, by using the eikonal approximation for pion distortion, rates to $^{12}_\Lambda$C states comparable to those calculated for capture from d orbits. Although the cascade calculation[23] based on the K⁻-^{12}C x-ray transition intensities reported since[24] rules out a non-negligible fraction for captures from s orbits [see Eq. (49)], we would like to comment briefly on this possibility, because mesic s orbits are fairly easy to reach once the standard assumptions behind a normal cascade process cease to hold. Using the K⁻ atomic wave function generated by the optical potential (i) and pion distortion parameter sets (b) and (c), we find 1⁻ rates smaller than in Table XIX by a factor of 2 and smaller than that given in Ref. 9 by a factor of 8. The summed (0⁺ + 2⁺) rates are a factor of 2.5–3 smaller than in Table XIX and a factor of 5 smaller than in Ref. 9. Set (a) gives $1s_\Lambda$ and $1p_\Lambda$ rates several times smaller than (b) and (c) give. This suppression of the calculated Λ-hypernuclear rates occurs due to the combination of a realistic K⁻ atomic wave function and of pion distorted waves fitted to π^--^{12}C scattering, an effect overlooked in Ref. 9. We have explained in Sec. III D the mechanism for the similar suppression of $^{12}_\Lambda$C*(0⁺) production in capture from p orbits (see the discussion of Table XV in Sec. IV B). Here we find an even stronger suppression effect in capture from s orbits, embracing now also the 1⁻ and 2⁺ rates. The general conclusion to be drawn from this trend is that captures from d orbits offer in ^{12}C the strongest rates for producing $^{12}_\Lambda$C states. To further escape the consequences of pion damping in the calculation of Λ-

hypernuclear production rates, one would have to invoke captures from $L > 2$ K⁻-^{12}C atomic orbits. However, captures from f ($L = 3$) orbits can already be safely neglected because the normal dipole x-ray transitions $f \to d$ will always win in ^{12}C over strong-interaction capture, and higher values of L ($L > 3$) are certainly incapable of reversing these systematics.

C. $^{16}_\Lambda$O

The $^{16}_\Lambda$O spectrum in the reaction (3b) gives evidence[12] for some structure involving one or two peaks for $T_{\pi^-} \sim 163$ MeV. The rates of production for the most obvious $^{16}_\Lambda$O* excitations expected in this energy range, $(p_{1/2}^{-1}, p_{1/2})0^+$ and $(p_{1/2}^{-1}, p_{3/2})2^+$, were calculated and reported (per Λ) in Sec. IV C, Table XVI. To convert to rates per stopped K⁻, we follow the same procedure applied to $^{12}_\Lambda$C excitations in the preceding subsection and multiply the rates per Λ by 0.070 from Table I and by 1.35 from Table XVII, disregarding the moderate changes expected for these quantities in going from capture in ^{12}C to capture in ^{16}O. The resulting calculated rates per stopped K⁻ for pion parameter set (d) are then given by

$$R(0^+)/K^- = 0.41 \times 10^{-4} ,$$
$$R(2^+)/K^- = 1.27 \times 10^{-4} , \tag{58}$$

with a substantial uncertainty that is best estimated by studying the sensitivity of the calculated rates in Table XVI to the pion-distortion parameter set used. The rates (58) are weaker than the rates calculated in ^{12}C for the $1p \to 1p$ transitions However, the data[12] are too inconclusive to allow a direct comparison with at this stage.

VI. CONCLUSIONS

We presented DWIA calculations of (K⁻,π±) yields, mostly on ^{12}C, for K⁻ captured from atomic orbits. The DWIA method was shown[10] to work well for (K⁻,π⁻) reactions in flight to the Λ-hypernuclear region and one expects a similar degree of success in the capture calculations. Accepting the validity of the DWIA, we found, however, substantial sensitivity of the calculated capture rates to the Λ-hypernuclear region to the pion distortion entering these calculations. This sensitivity would seem to detract from the prospects[4] of exploring Λ-hypernuclear spectroscopy in capture from rest, short of merely establishing new states (e.g., $1s_\Lambda$ ground states) hitherto unknown.

The validity of the DWIA for Λ-hypernuclear production was questioned by Hüfner *et al.*,[9] who argued that two-step processes in which a Σ is first produced and subsequently converts into a Λ are as strong as the direct one-step Λ production. However, these strong two-step processes are known to be almost exclusively accompanied by a π^- of energy typical to the Σ-hypernuclear region (Fig. 1 of Ref. 18). By focusing on the faster pions, with $q(\pi^-) \geq 220$ MeV/c in ^{12}C, one ensures the dominance of the one-step direct Λ production and thereby the validity of the DWIA.

Regarding Σ-hypernuclear production, the DWIA seems in place and we believe that the calculations are not

particularly sensitive to numerous details such as pion distortion, K^- cascade history, and binding effects. Yet, the state of the art in understanding why the observed Σ-hypernuclear levels are relatively narrow is not satisfactory, and doubts may be cast on the use we made of *real* bound-state Σ wave functions in the calculations reported here. We checked that by using complex unstable-bound-state[37] wave functions for the $1p(\Sigma^-)$ state, the 0^+ and 2^+ calculated rates in $^{12}_{\Sigma}Be$ increase each by about 70% if the decaying-state normalization $\int_0^\infty u^2(r)dr = 1$ is adopted. However, one encounters then difficulties in figuring out the normalizing "denominator" in expressions such as Eq. (22). This problem deserves further studies.

*On leave of absence from the Hebrew University, Jerusalem, Israel.

[1]T. Yamazaki et al., Phys. Rev. Lett. 54, 102 (1985).

[2]Proceedings of the International Symposium on Hypernuclear and Kaon Physics, Brookhaven, September, 1985, edited by R. E. Chrien [Nucl. Phys. A450 (1986)].

[3]M. A. Faessler et al., Phys. Lett. 46B, 468 (1973).

[4]T. Yamazaki, T. Ishikawa, K. Yazaki, and A. Matsuyama, Phys. Lett. 144B, 177 (1984).

[5]H. Tamura et al., Phys. Lett. 160B, 32 (1985).

[6]J. Žofka, Nucl. Phys. A450, 165c, (1986); see also R. Hausmann and W. Weise, Z. Phys. (in press).

[7]C. B. Dover, A. Gal, L. Klieb, and D. J. Millener, Phys. Rev. Lett. 56, 119 (1986).

[8]T. Yamazaki et al., Nucl. Phys. A450, 1c (1986).

[9]J. Hüfner, S. Y. Lee, and H. A. Weidenmüller, Phys. Lett. 49B, 409 (1974); Nucl. Phys. A234, 429 (1974).

[10]E. H. Auerbach et al., Phys. Rev. Lett. 47, 1110 (1981); Ann. Phys. (N.Y.) 148, 381 (1983).

[11]C. B. Dover, A. Gal, and D. J. Millener (unpublished); see also D. J. Millener, Nucl. Phys. A450, 199c (1986).

[12]R. H. Dalitz, D. H. Davis, and D. N. Tovee, Nucl. Phys. A450, 311c (1986).

[13]G. Bohm et al., Nucl. Phys. B24, 248 (1970); M. Jurić et al., Nucl. Phys. B47, 36 (1972); A. Montwill et al., ibid. A234, 413 (1974); T. Cantwell et al., ibid. A236, 445 (1974).

[14]A. Matsuyama and K. Yazaki, Hypernuclear Formation by Stopped Kaons, cont. M25 to the Tenth International Conference on Particles and Nuclei, Heidelberg, 1984, edited by F. Güttner, B. Povh, and G. zu Putlitz (MPI, Heidelberg, 1984).

[15]E. V. Hungerford, Nucl. Phys. A450, 157c (1986).

[16]A. Gal, Nucl. Phys. A450, 23c (1986).

[17]C. Vander Velde-Wilquet et al., Nuovo Cimento 39A, 537 (1977).

[18]C. Vander Velde-Wilquet et al., Nuovo Cimento 38A, 178 (1977).

[19]We follow the angular-momentum convention of A. de Shalit and I. Talmi, Nuclear Shell Theory (Academic, New York, 1963).

[20]C. J. Batty, Nucl. Phys. A372, 418 (1981).

[21]C. W. de Jager, H. de Vries, and C. de Vries, Atomic Data Nucl. Data Tables 14, 479 (1974).

[22]We are grateful to Dr. E. Friedman for allowing us to use his computer programs.

[23]G. T. A. Squier and C. J. Batty, private communication; we are grateful to Dr. C. J. Batty for providing us with the results of these cascade calculations.

[24]G. Backenstoss et al., Nucl. Phys. B73, 189 (1974); C. E. Wiegand and G. L. Godfrey, Phys. Rev. A 9, 2282 (1974).

[25]E. Friedman and A. Gal, Nucl. Phys. A345, 457 (1980).

[26]J. A. Carr, H. McManus, and K. Stricker-Bauer, Phys. Rev. C 25, 952 (1982).

[27]E. Friedman, private communication.

[28]M. Blecher et al., Phys. Rev. C 28, 2033 (1984).

[29]J. Piffaretti et al., Phys. Lett. 71B, 324 (1977); H. A. Thiessen et al., LAMPF Report No. LA-7607-PR, 1978 (unpublished) and C. J. Harvey et al., LAMPF Report No. LA-UR-84-1732, 1984 (unpublished).

[30]We are grateful to Dr. E. Boschitz for providing us with tables of $\pi^\pm$-^{16}O differential cross sections as measured at SIN by J. P. Albanese et al., Nucl. Phys. A350, 301 (1980).

[31]D. Ashery et al., Phys. Rev. C 23, 2173 (1981).

[32]R. H. Dalitz and A. Gal, Phys. Lett. 64B, 154 (1976).

[33]S. Cohen and D. Kurath, Nucl. Phys. A101, 1 (1967).

[34]A. Matsuyama, private communication.

[35]We are grateful to Dr. T. Yamazaki for informing us that this indeed is the case, and for providing us with a report by M. Iwasaki et al. on the formation of $A = 12$ hypernuclear systems from K^- absorption at rest in $(CH)_n$.

[36]D. H. Davis, private communication.

[37]A. Gal, G. Toker, and Y. Alexander, Ann. Phys. (N.Y.) 137, 341 (1981); C. J. Batty, A. Gal, and G. Toker, Nucl. Phys. A402, 349 (1983).